Materials Combustion Testing and Combustion Product Sensor Evaluations in FY12

Marit E. Meyer
NASA John H. Glenn Research Center
Cleveland, OH 44135

Paul D. Mudgett
NASA Johnson Space Flight Center
Houston, TX

Steven D. Hornung and Mark B. McClure
NASA White Sands Test Facility
Las Cruces, NM

Jeffrey S. Pilgrim
Vista Photonics, Inc.
Santa Fe, NM

Victoria Bryg
National Center for Space Exploration Research
Cleveland, OH 44135

Darby Makel
Makel Engineering
Chico, CA 95973

Gary A. Ruff and Gary Hunter
NASA John H. Glenn Research Center
Cleveland, OH 44135

NASA Centers continue to collaborate to characterize the chemical species and smoke particles generated by the combustion of current space-rated non-metallic materials including fluoropolymers. This paper describes the results of tests conducted February through September 2012 to identify optimal chemical markers both for augmenting particle-based fire detection methods and for monitoring the post-fire cleanup phase in human spacecraft. These studies follow up on testing conducted in August 2010 and reported at ICES 2011. The tests were conducted at the NASA White Sands Test Facility in a custom glove box designed for burning fractional gram quantities of materials under varying heating profiles. The 623 L chamber was heavily instrumented to quantify organics (gas chromatography/mass spectrometry), inorganics by water extraction followed by ion chromatography, and select species by various individual commercially-available sensors. Evaluating new technologies for measuring carbon monoxide, hydrogen cyanide, hydrogen fluoride, hydrogen chloride and other species of interest was a key objective of the test. Some of these sensors were located inside the glovebox near the fire source to avoid losses through the sampling lines; the rest were located just outside the glovebox. Instruments for smoke particle characterization included a Tapered Element Oscillating Microbalance Personal Dust Monitor (TEOM PDM) and a TSI Dust

Trak DRX to measure particle mass concentration, a TSI PTrak for number concentration and a thermal precipitator for collection of particles for microscopic analysis. Materials studied included Nomex®, M22759 wire insulation, granulated circuit board, polyvinyl chloride (PVC), Polytetrafluoroethylene (PTFE), Kapton®, and mixtures of PTFE and Kapton®. Furnace temperatures ranged from 340° to 640° C, focusing on the smoldering regime. Of particular interest in these tests was confirming burn repeatability and production of acid gases with different fuel mixture compositions, as well as the dependence of aerosol concentrations on temperature.

I. Introduction

NASA's ongoing collaborative efforts to develop early fire detectors and post-fire cleanup equipment include characterizing the smoke generated by common spacecraft materials. Understanding the most likely gas and aerosol fire signatures on a spacecraft is fundamental to the design of a fire protection system. Initial testing at WSTF in 2010 focused on developing a consistent post-fire challenge for the purpose of requirements definition and qualification of post-fire cleanup protective breathing equipment [1]. Subsequent testing in 2011 added instruments to characterize the smoke aerosol particles as well. Further work took place in 2012 with two additional test campaigns at the NASA White Sands Test Facility (WSTF). Multiple entities participated, bringing newly developed and mature gas sensors and aerosol instruments. These latest testing activities have benefitted from improvements to the test facility itself. Test matrices were broadened with the investigation of new fuels and various fuel preparation methods.

II. Test Facility and Procedures

The test facility consists of an exposure chamber, a custom smoke generator, and reference instruments. Several types of fuel samples have been developed and used in this test program as well as specialized test procedures. These are discussed in the following sections as well as the diagnostics specifically included for this test program.

A. Exposure Chamber and Smoke Generator

An instrumented chamber was developed for this testing. The chamber, shown in Figure 1 has a volume of 623 L (22 ft^3) with support plumbing to exhaust the chamber to a roof vent stack, as well as two fans to circulate the chamber atmosphere. The circulation fans are controlled through the data system and used during each test. Tests were conducted in ambient air at 12.4 psia (WSTF ambient atmospheric pressure). The chamber has ports for withdrawing samples and accommodating power and data cables. Figure 2 is a schematic representation of the instrumentation used in the testing.

The smoke generator,also shown in Figure 1, consists of a quartz-lined electrical tube heater with an air supply line that introduces a low flow of air to the hot mixture. This system has been designed so that both flaming and smoldering fires can be simulated. Several different smoldering conditions, which typically have the highest production rate of toxic products, were run in this test by operating the tube heater at specific set-point temperatures between 350 to 640 ^oC. In general, these scenarios emulate 1) a low temperature fire that produces a maximum of volatile organic compounds with little thermal oxidation, 2) a higher temperature test where the conditions produce a significant concentration of carbon monoxide (CO), and 3) a condition that produces the worst-case particulate concentration. Flaming conditions are simulated as a variant of the high temperature smoldering challenge where the effluent is intentionally ignited remotely after smoke production is well established. Furnace temperature control was improved for the current testing by adding a feedback temperature controller with a user selectable heating rate. Additional ports were added to improve chamber access and accommodate additional external sensors.

B. Sample Materials and Conditions

The experimental design has "evolved" somewhat with each test as we learn how to conduct this type of testing in an efficient way. Each test campaign was limited to 1 week, which forced us to be economical in choosing the fuels, parameters and replicates. The week-long tests carried out in 2012 differed from the original test in August 2010 and from each other in several ways. Based on the 2010 results, the fuel mass was standardized at 0.5 g per burn. A somewhat different set of fuel materials was used in each test, but with significant overlap. For the

September 2012 test, to enable complete burns, we decided not to pelletize the fuel; rather, loose granulated material was placed carefully on the mica liner and inserted into the oven.

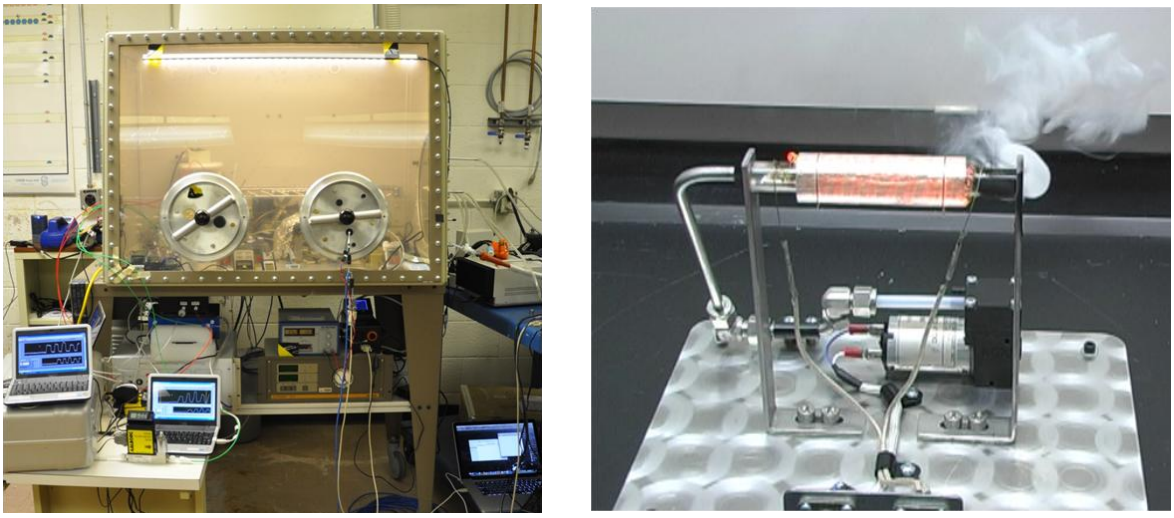

Figure 1. Exposure chamber during September 2012 testing (left), Smoke generator (right).

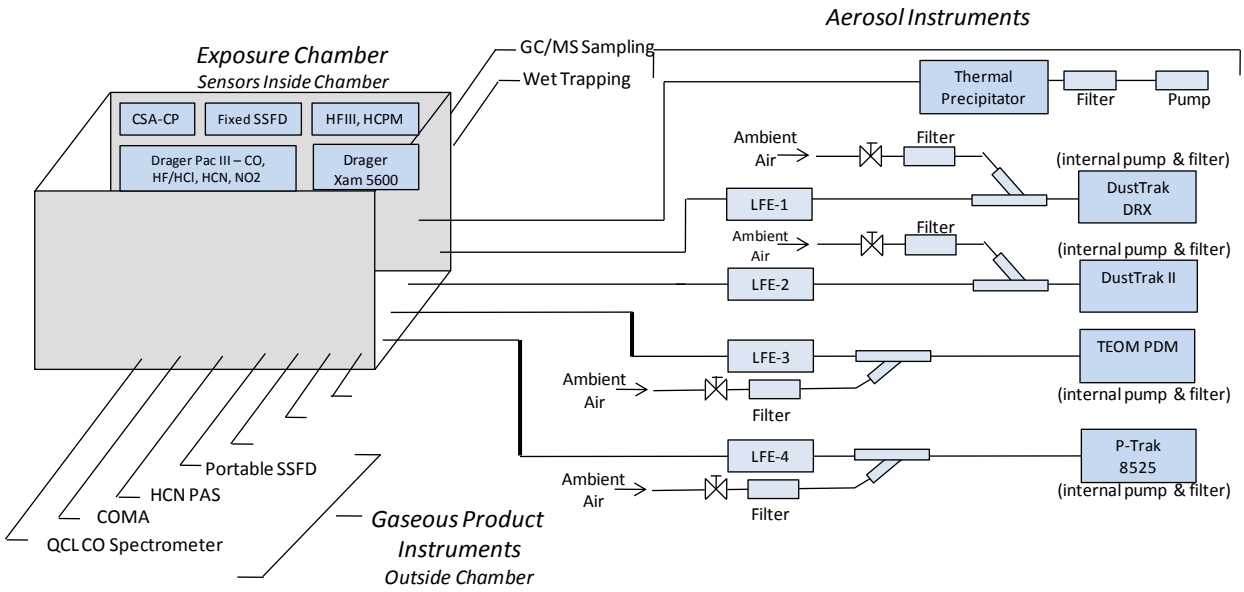

Figure 2. Schematic of instruments placed inside and plumbed to the chamber, including laminar flow elements (LFE) for dilution of aerosol instruments.

Tables 1 and 2 show the test matrices from the two test campaigns in 2012. Differences in the temperatures, materials, number of replicates and total number of runs indicate the evolution of the WSTF testing efforts and emphases. The Standard Mix fuel is a mixture of twelve granulated constituents represented in specific mass fractions down to the hundredth of a gram. Exact proportions and materials are outlined in Reference 2. This material was created as a fire fuel proportionally representative of materials on spacecraft. This fuel was predominantly used in February/March testing and in previous WSTF test campaigns [2]. Materials used for the February/March test are shown in Table 1. The PFPI wire insulation is partially fluorinated polyimide manufactured by TRW. The circuit board was a downgraded flight spare fully populated with certified conformal coating as an example of modern electronics. Materials for the September testing are shown in Figure 3. For the Sep 2012 test, we researched the current spacecraft wire specification and found it to be Mil Spec M22759, produced by using a

PTFE and polyimide tape wrap process to produce layers over the conductor which are then thermally fused. The insulation was stripped from 12 gauge M22759/86 wire (manufactured by Nexans) in short random lengths, and used as-is without further granulation. The Nomex cloth was scissors cut into 3 to 5 mm shredded pieces. PTFE granules were made with a rotary shaving device, whereas the PTFE powder was purchased, with a uniform size of 100 μm. The Kapton pieces were thin strips of film cut into approximately 2 mm squares. The Kapton film was difficult to shred and required some hand sorting to eliminate larger pieces. The granulated circuit board was made with a rotary grinder and metal portions of the circuit card assembly were avoided during the grinding process and in weighing out the 0.5 gram samples to avoid skewing the weight of the 0.5 g sample.

Table 1. Feb-Mar 2012 Test Outline (some ignition)

Material (0.5 g)	Furnace Temp/C	Ignite	Replicates	# Tests	Notes
Standard Mix	340,440,540,640	Yes	1-2	7	Granulated, see Reference 2
Granulated Circuit Board	340,440,540	Yes	2-3	5	Populated, conformal coated
PFPI wire insulation	540,640	No	3-4	7	20AWG stripped
100% PTFE	540,640	No	2-3	5	Granulated
100% Kapton	540,640	No	2-3	5	Granulated
50:50 PTFE/Kapton mix	540,640	No	1-2	3	Mixtures of above
25:75 PTFE/Kapton mix	540,640	No	2	4	
75:25 PTFE/Kapton mix	540,640	No	1-2	3	
10:90 PTFE/Kapton mix	640	No	2	2	
90:10 PTFE/Kapton mix	640	No	2	2	
			Total Runs:	**43**	

Table 2. Sep 2012 Test Outline (No ignition)

Material (0.5g)	Furnace Temp/C	Replicates	# Tests	Notes
Nomex	640	7	7	HT9040, natural, untreated
Nexans Wire Insulation	640	6	6	M22759/86 12AWG stripped
100% PTFE	640	8	8	4 Granulated & 4 powdered PTFE
100% Kapton	640	5	5	Granulated
PTFE/Kapton mixes	640	3-4	18	10/90; 90/10; 25/75; 75/25;50/50
Circuit Board (PCB)	340,440,540,640	2	8	Granulated
PVC	640	1	1	Granulated; for HCl production
PCB+PVC	640	3	3	0.5g PCB with 0.05g PVC "std addition"
PCB+PVC	640	2	2	0.5g PCB + 0.1g PVC
PTFE+PVC	640	1	1	0.4g PTFE + 0.1g PVC
		Total Runs:	**62**	

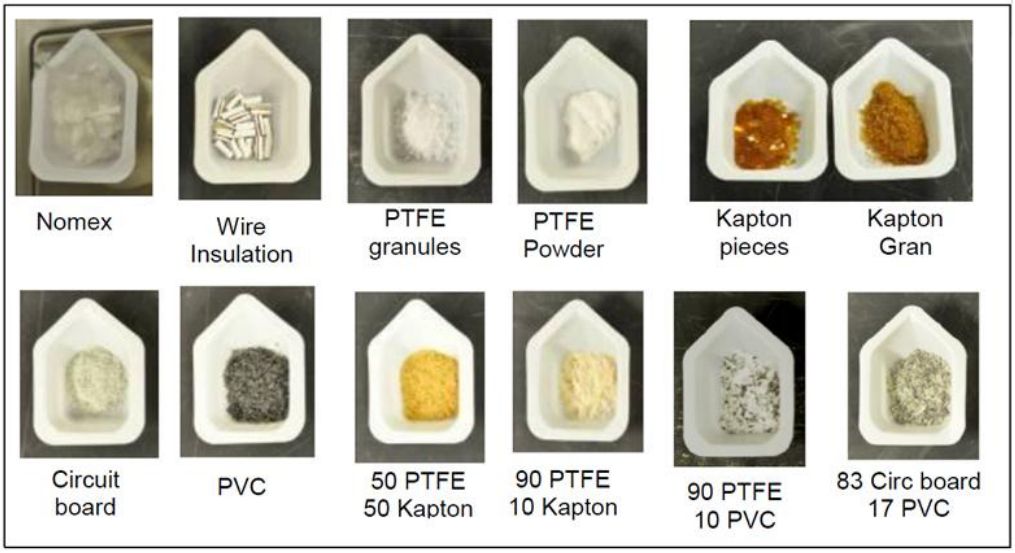

Figure 3. September sample materials before burning.

C. Test Procedure

The sample tube heater near the center of the chamber is controlled by a LabView interface which dictates the temperature ramp duration and magnitude. The test procedure timing is outlined in Table 3. A fan near the rear corner is turned on for approximately 30 seconds after the heater is turned off to provide a uniform concentration inside the test chamber. After mixing, the combustion products are allowed to decay for 5-10 minutes after which the chamber is purged with a vent fan. The front ports are opened to allow fresh lab air to be pulled into the chamber during venting. The time to complete a test, from the chamber sealing until the final venting is approximately 20-30 minutes.

Table 3. Standardized Test Procedure Timing (each run)

Step	Description
1	Load fuel, close up chamber, turn off purge vent
2	Ramp furnace temperature up to target temperature
3	Turn furnace blower ON once furnace temperature reached (at t=3 min)
4	Hold furnace temperature for ~ 4min
5	Turn off furnace at t=7 min & stir chamber via muffin fan for 30 sec
6	5 to 10 min dwell/natural decay (occasionally longer)
7	Vent chamber, switch on purge duct fan
8	Remove and weigh ash

III. Test Instrumentation

A record number of sensors were incorporated in the testing campaigns of 2012. Table 4 lists each instrument and identifies its core technology. The source of each instrument is either the designer or manufacturer and the sponsoring NASA organization that facilitated participation in the WSTF testing. Not all instruments were present both in February/March and September testing and improvements were made to some in between testing campaigns.

Table 4. Test Instrumentation

Instrument	Source	Core Technology	Target Analytes
PAS	Vista Photonics/GRC	Photoacoustic TDLS*	HCN
HFIII, HCPM	Vista Photonics/GRC&JSC	Enhanced TDLS	HF, HCl
COMA	Vista Photonics/GRC	Multipass TDLS	CO with CH4 compensation
SSFD Fixed unit	Makel Engineering/GRC	Solid state sensor	CO, CO2, hydrocarbons (HC)
SSFD Portable unit	Makel Engineering/GRC	Solid state sensor	CO, CO2, hydrocarbons (HC)
CSA-CP	Industrial Scientific/JSC	Electrochemical cell	O2, CO, HCN, HCl
Xam-5600	Draeger/JSC	Electrochemical cell/NDIR	O2, CO, HCN, CO2
PacIII	Draeger/WSTF	Electrochemical cell	CO, HF/HCl, HCN, NO_2
Thermal Precipitator	GRC	Particle thermophoresis	Aerosol capture for microscopy
TEOM PDM	ThermoFischer/GRC	Gravimetric	Aerosol mass concentration
DustTrak DRX	TSI, Inc./GRC	Laser photometer, with single particle counting	Aerosol mass concentration
DustTrak II	TSI, Inc./WSTF	Laser photometer	Aerosol mass concentration
P-Trak 8525	TSI, Inc./WSTF	Condensation/Light Scattering	Ultrafine particle concentration
GC/MS**	Hewlett Packard/WSTF	Gas chromatography/mass spectrometry	Volatile organic compounds
Ion Chromatography	WSTF	Offline IC, wet trap sample analysis	Inorganic anions
Quantum Cascade Laser Spectrometer***	Port City Instruments/JPL	Multipass TDLS	CO

*Tunable diode laser spectroscopy **GC/MS data not included ***This spectrometer is not described here

A. Tunable Diode Laser Spectroscopy based instruments from Vista Photonics

An improved photo-acoustic (PAS) based HCN sensor was present at both rounds of WSTF testing in 2012. This sensor is superior to the earlier FY2010 PAS instrument which operated at 1531 nm [3]. That sensor read

significantly higher HCN levels than other available diagnostics under the test conditions. It appeared that other, as yet unknown, combustion evolved hydrocarbon species were contributing to the HCN measurement. In contrast, the new PAS sensor operates at 2498 nm where fewer hydrocarbons can interfere with HCN measurement. The PAS gas sensor cell was thermoelectrically heated to a fixed temperature in order to maintain a stable acoustic resonance frequency. The laser diode was simultaneously wavelength modulated and wavelength scanned by injection current over the line center of the gas target absorption feature. The laser wavelength was modulated at the 3 kHz cell resonance frequency. Absorption of laser emission by the target gas is converted to sound occurring at the modulation frequency, which is the natural resonance frequency of the acoustic cell. The cell resonance provides about an order-of-magnitude improvement in sensitivity over non-resonant operation. Measurement precision for HCN is about 0.3 part-per-million (ppm) with a linear averaging time of 20 seconds. Present testing has shown a much closer correlation with other HCN sensors, indicating that this new wavelength is unaffected by other combustion products.

Earlier PAS combustion measurements at WSTF have shown that optical approaches suffering long sample interaction times are not effective when applied to highly reactive transient evolved combustion species. In contrast, the present employed technique for reactive acid gases utilizes rapid sampling and short sample interaction paths in an SBIR-developed proprietary path length enhanced optical approach combined with wavelength modulation spectroscopy (WMS) and tunable infrared semiconductor laser diodes [4]. Several prototypes have been successfully demonstrated for monitoring hydrogen fluoride (HF) in testing at WSTF using distributed feedback (DFB) laser diodes. A companion effort recently demonstrated that like performance for hydrogen chloride (HCL) can be provided using a similar architecture. Two recent developments have enabled a *multi-gas* optical acid gas monitor with increased performance. 1) Demonstration of sub-parts-per-million (ppm) sensitivity for HCL at 1742 nm allows implementation in a common sample cell with the HF sensor operating at 1312 nm and using the same electronics. 2) The emergence of vertical cavity surface emitting laser (VCSEL) diodes at both wavelengths eliminates the need for fiber-coupled telecom devices which draw much more power and reduce portability. The new prototype device employed in the present WSTF testing combines VCSEL-based, real-time, high-performance concentration measurements with rapid sampling for both HF and HCL simultaneously. Little surface interaction is suffered as the gas samples need only traverse a few mm aperture to enter the optical cell and are directed across the aperture by a simple fan. A second Phase III-developed HF sensor, utilizing a fiber coupled DFB laser diode at 1312 nm, was also employed in the present testing. HF measurement precision is better than 0.1 ppm and HCL is better than 0.2 ppm.

A VCSEL-WMS sensor for CO utilizing a simple optical multipass cell was designed and built on a Phase II SBIR project (CO multipass analyzer, COMA). The delivered sensor version operates with a netbook computer (Mini 9, Dell). Although the sensor has already been operated with Field-Programmable Gate Array (FPGA) electronics during the Phase II project, the netbook based version is more flexible and allows easy change of sensor parameters. The netbook based version is more suited for WSTF testing due to its adaptability in the field. The sensor dimensions are 17.8 cm x 12.7 cm x 8.1 cm (not including the netbook). An FPGA based (stand-alone) CO sensor has similar dimensions. Note that the aim of the electronics development is to operate the CO sensor as an additional channel of an emerging Vista Photonics combined combustion products monitor (CPM). The sensor cell is designed for compactness and ruggedness. It has no moving parts; all components are solidly mounted. Cell dimensions are about business card size . In the developed sensor cell the laser is solidly attached to the cell at an angle. This angle is precisely machined into the cell. It determines the number of passes through the cell. Eight passes are realized in this cell leading to an absorption path-length of 63.6 cm. Measurements at WSTF were performed with a low-power, non-temperature stabilized sensor. Free-space single mode 2330 nm VCSELs are utilized in the COMA architecture. The VCSELs typically deliver about 0.3 mW of output power in single mode operation and are tunable from about 2333 nm to 2341 nm. CO measurement precision is about 0.5 ppm.

B. Fixed and Portable Smart Space Fire Detection System (SSFD)

Fixed and portable version of a Smart Space Fire Detection System (SSFD) developed by Makel Engineering, Inc. and NASA GRC were tested. Intial versions of these systems were tested in 2011 [5]. The SSFDS includes the core electronics, interfaces, microprocessor, and overall hardware architecture from the "Lick and Stick" technology developed for space flight leak detection applications and a fire detection system developed for aeronautics [5-6] .

The current generation of the SSFD sensor system provides the capability to detect CO, CO_2, O_2, H_2, and hydrocarbons while tracking temperature, pressure, and humidity. The individual solid state sensors are integrated into a single package that is approximately 17.8 cm wide x 10.2 cm long x 4.6 cm tall, excluding the external cable, with weight and power consumption near a 1 kg and 6 W respectively. There is an electrical connector for power and RS485 communication, but the system can be configured for wireless capability. The portable version of the device includes a touch screen LCD, sampling pump, and rechargeable battery. For the fixed system the sensor elements are exposed to the external environment by diffusion through stainless steel filters standardly used in combustion product monitoring, but are sealed internally from the rest of the electronics and enclosure. For the portable SSFD, a sample pump inside the unit pulls air to the enabling the system to used as a sniffer. The overall design of the unit enables the device to incorporate new sensor types and improved sensors for individual species with minimal rework of the unit. The modular electronics also enables upgrade and improvement to the hardware. The MEMS chemical sensor technology used in the both systms consists three different types of MEMS chemical sensor platforms resistors, solid state electrochemical cells, and Schottky diodes. Each sensor type or platform provides very different types of information on the environment and is meant to have limited cross-sensitivity (i.e., be orthogonal in its response). Integration of the information from these orthogonal sensors can provide increased whole-field information on the environment. The approach is to give quantitative readings of the species of interest. The current generation of the systems tested included specific improvements to CO and CO_2 sensor sensitivity and stability. In addition, refined real-time algorithms for improving individual sensor selectivity were implemented. Thus, this testing employed the same core sensor technology, but integrated with different hardware platforms and implemented at different locations in the test environment. The data presented in this paper will concentrate on the results provided by two types of CO sensors in both a fixed position unit and a portable unit. One sensor is intended for low concentration measurements (Fixed-L and Portable-L) and is intended to also have use in environmental monitoring. The second type of CO sensor is intended have a broad range of detection capabilities extending into higher levels of CO concentration that may be present in some fire conditions (Fixed-H and Portable-H). Data from the other sensor technologies was also recorded and is available for future analysis and crosscorrelation.

C. Compound Specific Analyzer-Combustion Products (CSA-CP), Draeger X-am 5600, Drager Pac III

Several commercial multi-gas monitors were used in the test, including the Compound Specific Analyzer-Combustion Products (CSA-CP) from Industrial Scientific which is identical to that used on the International Space Station, and an X-am 5600 unit from Draeger. Both measure O_2, CO, and HCN electrochemically. Additionally, the CSA-CP measures HCl electrochemically and the X-am 5600 measures CO_2 by infrared detector. Both units were calibrated at Johnson Space Center in Houston prior to the test and checked at WSTF before and after the testing. The units were located front and center inside the chamber (see Figure 1) to be able to see the display and record the maximum concentrations during each test. Data were also automatically logged and downloaded after all testing was completed. The Draeger PacIIIs are single gas electrochemical monitors equipped with sensors for CO, HCN, and HF/HCL. These three units were also located near the front ports. Prior to testing these monitors where calibrated using commercial certified gas standards.

D. Aerosol Thermal Precipitator

A thermal precipitator was designed at Glenn Research Center to collect smoke aerosol particles for microscopic analysis. The design takes advantage of the thermophoretic force on a particle in a large temperature gradient created by opposing thermoelectric coolers and kapton heaters. The particles are driven to the cold side of the gradient, which in this device is set of SEM stubs prepared with a section of carbon tape and TEM grids to facilitate a variety of analyses. Information on particle morphology, size, chemical composition and agglomerate structure obtained from these tests supplements aerosol concentration data collected.

E. Tapered Element Oscillating Microbalance (TEOM) Personal Dust Monitor (PDM)

The TEOM is a direct-reading gravimetric aerosol instrument manufactured by Thermo Fisher Scientific that measures aerosol mass deposited on a filter. The filter is mounted on a hollow tapered glass stalk through which air is drawn and which vibrates at a frequency proportional to the mass on the filter. The system electronics monitor the frequency changes, and changes in mass on the order of micrograms are computed and recorded every 5 seconds. Aerosol mass concentration can be derived from the change in mass on the filter and the known volumetric flow rate of air through the filter. The PDM is a wearable respirable dust sampling version of the TEOM for use in mining and other hazardous occupations.

F. DustTrak DRX Monitor and DustTrak II

Aerosol photometers measure mass concentration by measuring the combined laser light scattered from many particles at once. Both DustTrak ™ monitors (TSI Inc.) are the same except the DRX combines ensemble scattering with single particle detection to provide real-time size-segregated mass fraction concentrations up to 150 mg/m^3. In this testing, aerosols below 1 μm in diameter are the predominant sizes however it is of interest in fire characterization to determine which fuels generate particles above this threshold. Optical aerosol instruments give a material-dependent response, with particle refractive index dictating the amount of light scattered. This instrument is factory calibrated with Arizona Road Dust for the wider market of occupational hygiene applications. A custom calibration for smoke was performed using a polydisperse mineral oil aerosol that resembles the size distribution of smoke.

G. P-Trak 8525

The P-Trak™ (TSI Inc.) is a condensation particle counter that measures aerosol number concentration. This device operates by passing the aerosol-laden particle stream through a region saturated with isopropanol vapor and then into a cooler region where the vapor condenses onto the particles increasing their diameter such that they can be readily counted by a light scattering device. This instrument is designed for the occupational hygiene market and operates over a range of 0 to 10^5 particles/cm^3 and 20 nm to 1 μm diameter. Dilution is required, since the smoke concentration is higher than the upper range limit.

H. GC/MS

A Hewlett-Packard®[1] 5890A Gas Chromatograph with a 5970 Series Mass Selective Detector was assembled to perform analyses of combustion products. The Gas Chromatography with Mass Spectral Detection (GC/MS) instrument was equipped with a 30-m x 0.53-mm ID x 5-μm phase 100-percent dimethyl polysiloxane capillary column, a VICI®[2] direct injecting 10-mL sampling loop, and a 6-port valve. To obtain a sample, a 12-ft heated transfer line, transfer line isolation valve, vacuum pump, and vacuum pump isolation valve were used to move the gas sample from the mask to the sampling loop. The inlet system is configured so that the vacuum pump evacuates the valve, loop, and heated transfer line to the transfer line isolation valve. The vacuum pump isolation valve is then closed and the heated transfer line isolation valve opened to pull in the gas sample to be analyzed. After the gas sample is pulled into the loop, the pressure is measured, the 6-port valve switched, and the gas sample injected onto the column.

I. Ion Chromatography

The wet-trap samples were acquired by pulling an air sample from the chamber over a sorbent wetted with deionized water at a measured air flow rate for a specific time. This sorbent was then desorbed into 10 mL of IC eluent, filtered then run on the ion chromatograph (IC). Chamber concentration of acid gas was calculated by flow rate, time, volume of water in the trap and concentration of the corresponding anion determined by the IC.

IV. Results and Discussion

With the exception of the GC/MS data, all of the results from the two testing campaigns are tabulated in the appendices. While all individual chemical parameters could be plotted and commented on, only select data are analyzed, plotted and discussed as examples or highlights for brevity. Photographs of the residual ash after testing are shown in Figure 4 and masses are given in Appendix E.

The goal of the testing, along with proving instrument performance, is to consider spacecraft fire characteristics, including gas and aerosol signatures. Many topics concerning the data merit their own dedicated study, however, some of the chemical and aerosol results are discussed here in light of ongoing WSTF testing and the sensors under development.

A. Particle Microscopy

As part of the particle characterization of smoke aerosols generated during two White Sands testing regimens, samples were collected via a thermal precipitator. The thermal gradient allows particles to collect on scanning electron microscopy (SEM) stubs and transmission electron microscopy (TEM) grids. A strip of conductive carbon

[1] Hewlett-Packard® is a registered trademark of Hewlett-Packard Development Company, Houston, TX.
[2] VICI® is a registered trademark of Valco Instruments Company, Inc., Houston, TX.

film was placed onto the surface of the SEM stub to allow for viewing of the particles on both the aluminum stub substrate as well as a neutral carbon background. TEM grids with a) contiguous carbon film as well as a b) holey carbon film were placed at the edge of the carbon film to allow sample collection for higher magnification examination. Observations about aerosol particle size and morphology are made with a Hitachi SEM and Philips TEM. Elemental information is gained by use of an EDAX energy dispersive x-ray analyzer (EDS) instrument on the SEM. The images shown here are typical of those generated by the heated samples.

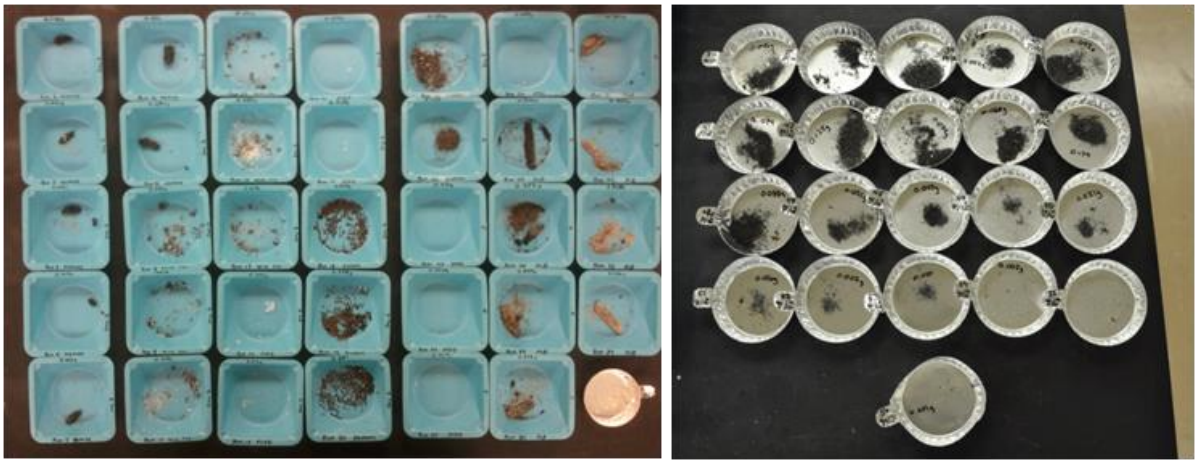

Figure 4. September sample ash after burning, arranged in chronological order of tests.

A 100% Teflon sample burned at 640 ^{o}C during February testing is shown in Figure 5. Teflon particles are generally spherical. Other areas on the 640 ^{o}C sample SEM stub (not pictured here) show evidence of acid pitting (potentially from HF), as well as the precipitated particles. The image on the left is a SEM image of precipitated particles and the center image is an elemental map showing fluorine (F) within the particles. It is interesting to note that the fluorine is still concentrated in the aerosol particles which indicates that the material did not decompose significantly during the test. Another indication that the Teflon is still intact is shown in the TEM image on the right where the Teflon particle exhibits a crystalline interior with an amorphous coating.

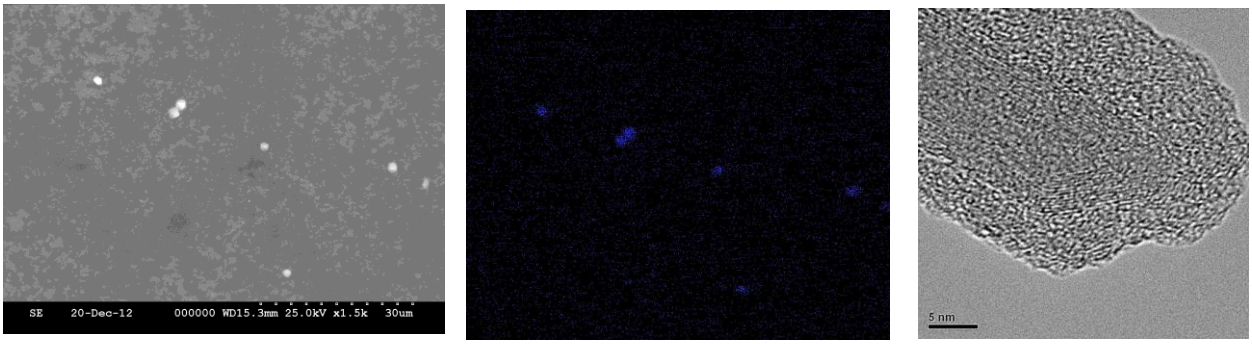

Figure 5. Teflon sample at 640^{o} C on SEM stub with map showing concentration of fluorine (center) and HRTEM image (right).

Figure 6 illustrates particles from the September tests. This is a sample of a circuit board at 640^{o}C. Circuit boards exhibit significant amounts of particle deposition. Elements detected within these particles include oxygen, copper, iron, silicon, and fluorine; a representative EDS spectra from this sample is shown on the right. The gold in the EDS spectra is from a coating sputtered onto the stub to prevent charging.

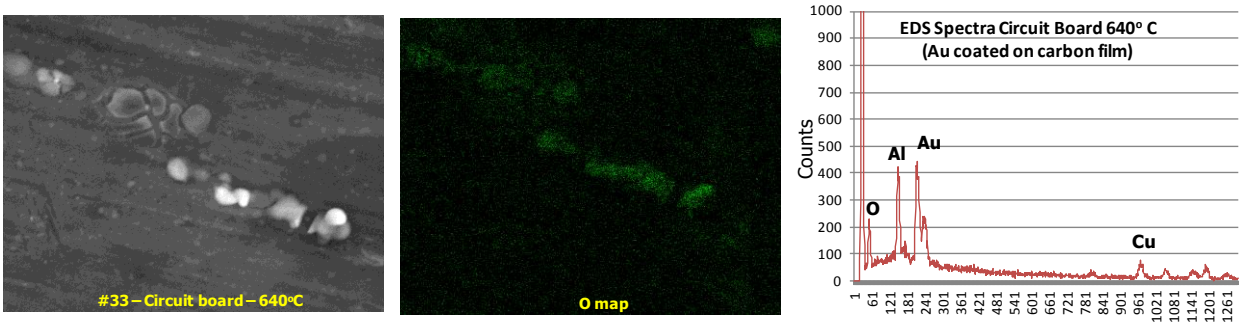

Figure 6. Circuit board sample at 640° C with map showing concentration of oxygen (center) and a typical EDS spectra (right).

Nomex particles were mostly spherical. EDS results indicate that Nomex aerosol particles contained bismuth, which is a heavy metal additive that increases flame retardancy and inhibits smoke generation. Particles captured from other sample materials were all mostly spherical with the exception of the Kapton, which exhibited string-like agglomerate structures. Figure 7 shows representative images of the wire insulation, Kapton and Teflon, all at 640° C. The thermal precipitator was not designed to capture particles for the purpose of generating a particle size distribution by microscopy. The design intent was to give insight into particle morphology and smoke repeatability, and there may be some size fractions that were not captured at all due to the limitations of the thermophoretic sampling process, fixed flow rate and other design parameters.

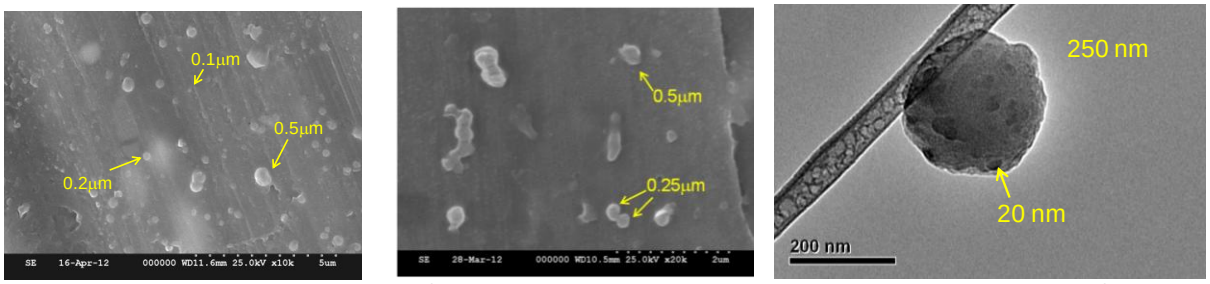

Figure 7. Wire insulation particles at 640° C are nearly spherical (left), some Kapton particles at 640° C exhibit chain-like agglomerate structure (center), a 640° C Teflon particle which is a compact agglomerate made up of nanoparticle primaries. The rod to which the particle adhered is the carbon film of the TEM grid.

B. Chemical Combustion Products: Select Results and Trends

A significant amount of data across multiple chemical sensor systems was collected during this testing. The Appendices briefly summarize the large amounts of raw data associated with various test runs. In general, there was notable consistency amongst the various sensor outputs although some variation was noted. Analysis of this data, evaluation of sensor system performance, and reasons for potential variations in sensor response is beyond the scope of this paper, and an appropriate subject for a separate paper. The purpose of this section is to give general trends and summarize some of the highlights of the data observed this testing.

Much of the chemical data (peak concentrations from all sensors for each run) from the September 2012 test (640° C without ignition) is reduced and displayed in Fig 8 as averages and ranges, although the PFPI wire insulation and Standard Mix data are from the Feb test. Figure 8 serves as a quick comparison chart and reference for gas production vs. material and is helpful in designing combustion experiments and sensor evaluations in a "relevant environment". The CO concentration range for Kapton was the widest for a single material, and PTFE the smallest. CO yield for PTFE was also smallest (9 ppm average). Mixtures (PTFE/Kapton indicated as mass percentages) gave interesting results. A small amount of Kapton added to PTFE dramatically increased CO and vice versa. Yield for M22759 wire insulation is similar in CO production to 90/10 PTFE/Kapton, whereas the PFPI wire insulation approaches that of 75/25 PTFE/Kapton. As expected the PTFE and PTFE containing fuels produce the

highest HF concentrations whereas materials like Nomex, containing no fluorine naturally do not produce HF. The PCB and Standard Mix produce little HF. The 2 different types of wire insulation gave similar average HF production with differing ranges. A small amount of Kapton in Teflon mixture appears to boost production of HF. Future work should include a study of the role of proton donor in HF production. As expected, Kapton is best producer of HCN and PTFE least (zero). Interestingly, a small amount of PTFE in Kapton seems to boost HCN production. The 4 ppm average HCN from M22759 wire insulation reflects the tape wrap style construction—a thin layer of polyimide between 2 layers of PTFE. PFPI wire insulation produces little HCN, although the backbone is polyimide. That observation along with the high HF signature indicates that "partially fluorinated" is actually a large degree of fluorination.

The September test was the first to detect HCL unequivocally from PVC and PVC-containing mixtures via TDLS. Presence of significant acid gases were confirmed via the wet trap ion chromatography results (see Appendix B & D). As an example, Fig 9 shows that acid gases persist in the chamber longer than expected—there is a spike in production then an initial rapid decay, in which HF/HCl are reacting with surfaces in the chamber, then a slow decay, with these toxic species persisting for 10's of minutes. It appears the surfaces become less accommodating for the acid gases during prolonged exposure. Note that the HF concentration never returns to zero between runs after the chamber has been exposed a few times. Run 13 (Fig 9 right) was allowed to run for an extended period, and results show HF still present after more than two hours. An exponential model would predict nearly complete decay of HF within about 20 minutes based on the initial, rapid, decay. Nonetheless, after 20 minutes the HF concentration is about four times higher than predicted by an exponential fit. This has implications for fire response on spacecraft and other closed inhabited environments and for combustion product monitor development.

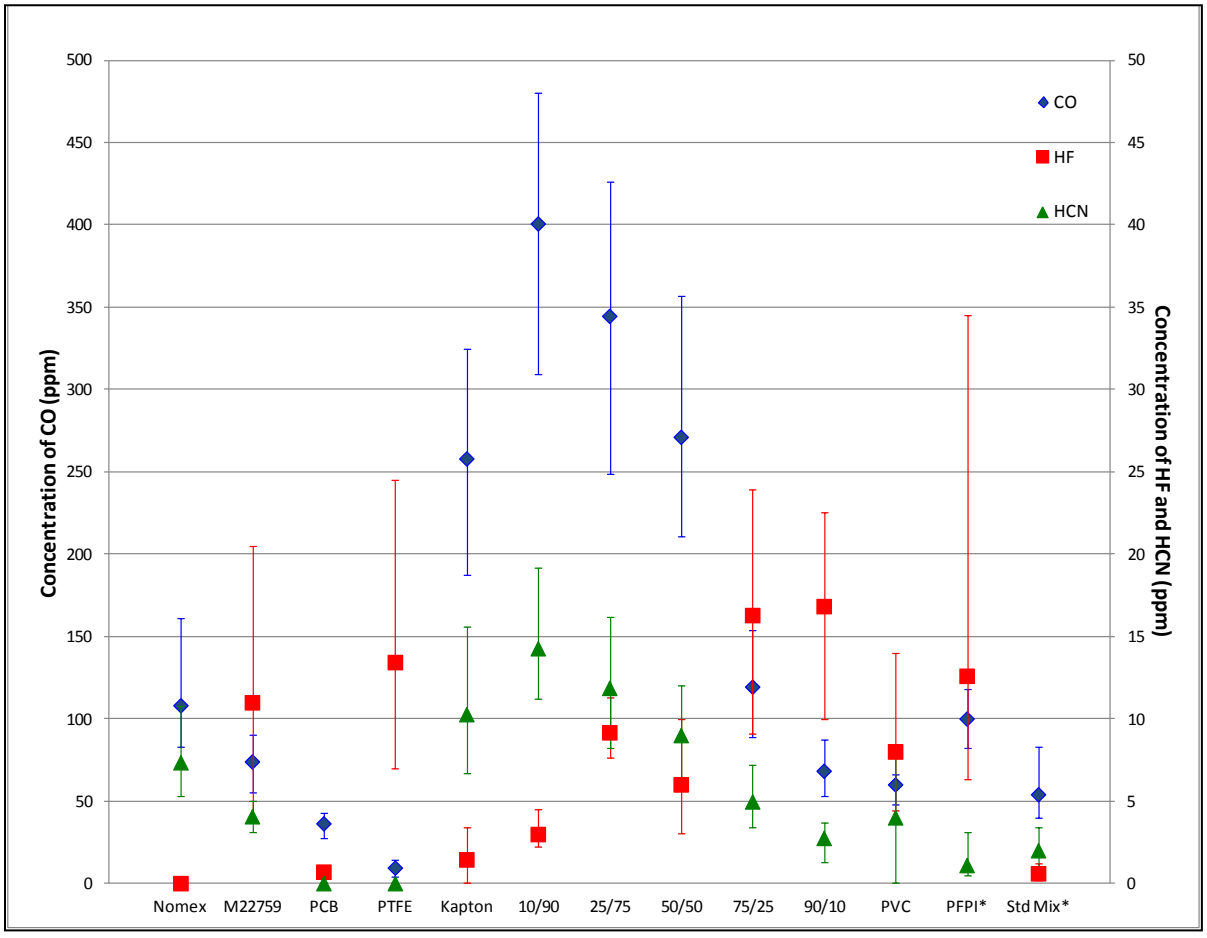

Figure 8. Range and Average of Maximum Concentration of Gas Products vs. Fuel Material at 640° C.

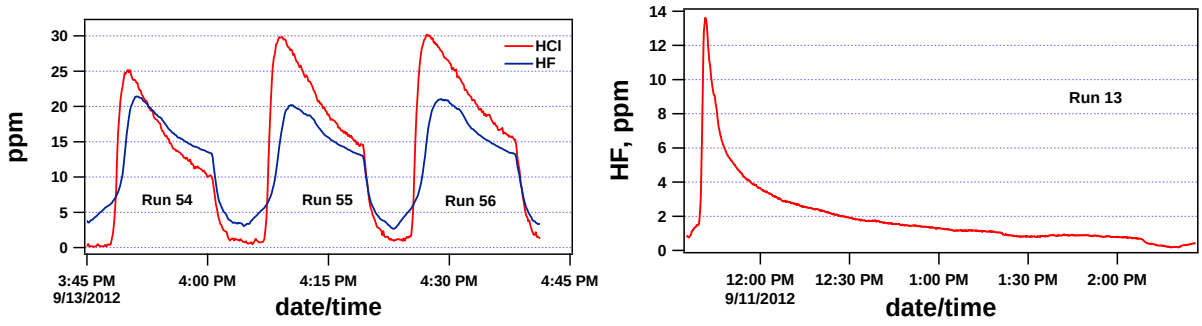

Figure 9. Production and persistence of HF and HCL from PTFE/PVC burns (Runs 54-56, Left), each with a short decay before venting the chamber, and HF from the burn of M22759 wire insulation (Run 13, Right) which was intentionally left to decay for approximately 3 hours.

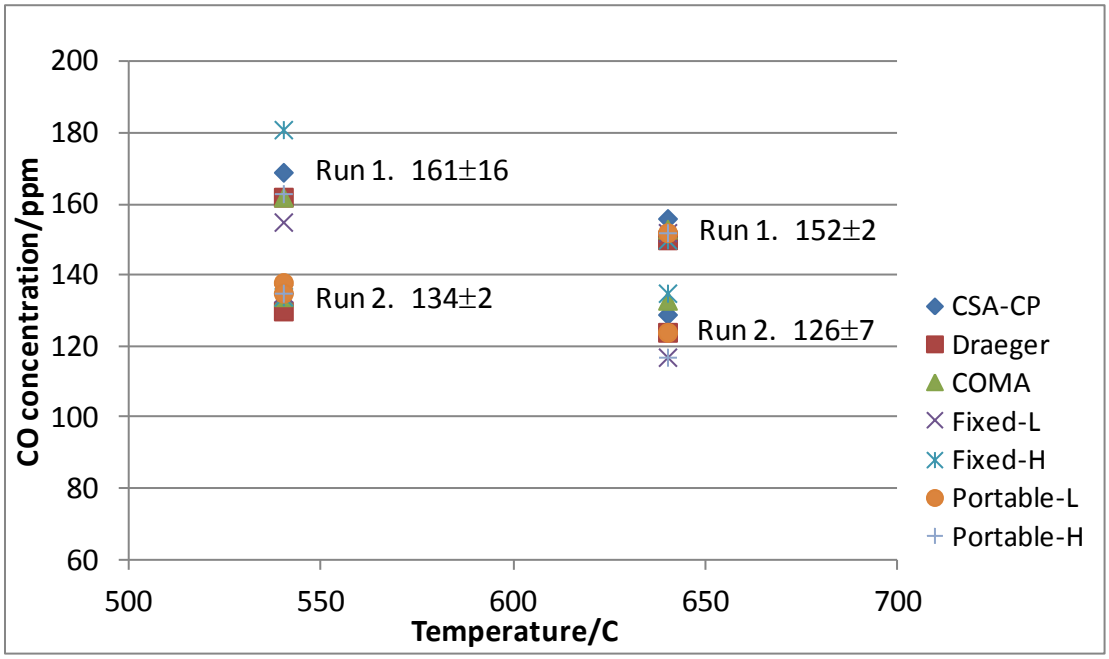

Figure 10. Comparison of CO sensor performance for Kapton at 2 burn temperatures (February/March).

Different sensor technologies were compared in the tests with standard commercial units. Figure 10 illustrates one such analysis-- the maximum CO values from all sensors in Kapton runs during the February/March test, which showed remarkable precision with all sensors reporting CO within 10% of the mean for a given run. Results varied between runs, but that was a function of other factors--studied in a little more depth in the September test. The Sept 2012 test sequence was our most recent and most well controlled, so it is the best data for which to discuss run-to-run variability (reproducibility) for the current practice. The September data in Appendices C and D includes calculated average and standard deviation. Based on the CO results, the run-to-run reproducibility within a given material, with the exception of PTFE, ranged from 12.5 to 18% relative standard deviation (RSD). The M22759 wire insulation had the lowest RSD for CO at 12.5%, indicating best reproducibility as measured by all the CO sensors. The RSD for PTFE was about double (29%), but that is likely from the fact that the CO yield is low for PTFE (9 +/- 3 ppm). The run-to-run RSD for HCN from Nomex was about 20% and that for M22759 wire insulation was 15.3%, which indicates decent reproducibility in terms of HCN, despite the lower yields. Because

the acid gas yield was generally also much less than CO (except for PTFE) and more reactive than CO and HCN, the RSDs tend to be higher for HF and HCl, thus less useful for assessing run-to-run variation.

1) Fuel Preparation Effects

Testing in February/March involved mostly pelletized fuel. This was the approach taken for the early fire cartridge testing process in 2010 and had persisted for subsequent campaigns. The standard mix had variation in the textures of the constituent materials that the pellet provided a consistent starting configuration. Some materials retained the pellet shape throughout the burn whereas other materials collapsed into granules, providing more available surface area. When the pellet remains intact, the thermal decomposition mechanism may be altered by the presence of a char front that progresses into the pellet over the duration of the test. Combustion products generated at the char front must traverse the surrounding ash in order to be liberated. This process was never rigorously investigated, however, in order to remove this variability between fuel materials, the second round of testing was performed without the pellet press. Thus all the fuels had a larger surface area available for thermal decomposition.

Less HF from Pelletized Fuel versus Powder

The pelletized blends of PTFE and Kapton produced significantly lower levels of HF than the loose mixtures as determined by the identical HF optical sensor placed in the same relative proximity to the combustion source. While the two rounds of testing occurred about 6 months apart for the pelletized samples and the loose samples, relatively good agreement was obtained for wire insulation samples under the same test conditions (e.g. 640^{o} C). Figure 11 presents the wire insulation samples average HF production over multiple replicates as a horizontal line. Although different types of wire, note the good agreement from the two rounds of testing for the wire insulation regardless of whether the sample was pelletized or loose. It stands to reason that the wire insulation is already well mixed due to the nature of its construction and that pelletized or loose grouping of the insulation does not significantly impact surface interaction effects which are those likely responsible for promoting HF production. Importantly, there is a significant difference in HF promotion based on whether the blended samples are pelletized or loose. Indeed, the pelletized blends, regardless of mixture fraction, never produce as much HF as the pelletized wire insulation. In contrast, the higher PTFE fractions in the loose mix produce more HF than that produced by the loose wire insulation. This is strong evidence for the importance of surface and localized gas phase interactions between the PTFE and Kapton materials in producing HF. The wire insulation produces high levels of HF in both cases and provides large surface interaction between the two materials. Likewise, the loose mixtures may produce more HF because of the blurring of inside versus outside interactions produced by the pellet arrangement. The loose material also likely heats up more uniformly over a greater surface area than the pelletized material. For larger PTFE fractions the wet trap results (Fig 11) are significantly higher, perhaps indicating there are other fluorinated products that hydrolyze and yield additional fluoride in the wet trap.

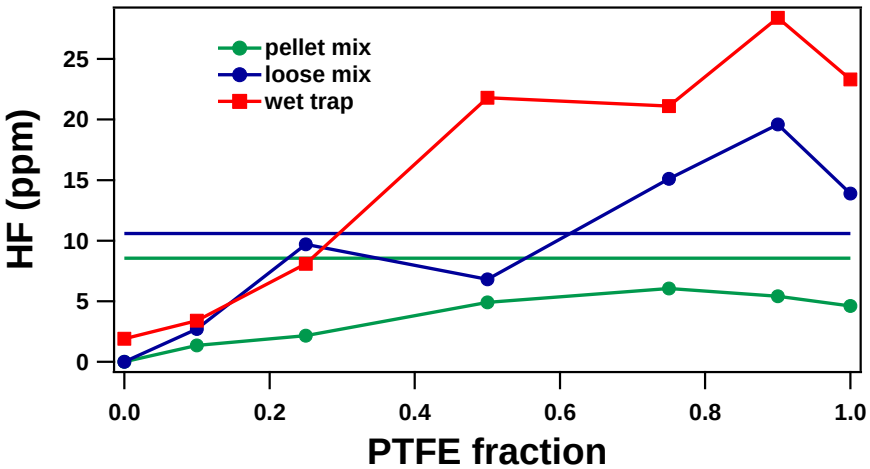

Figure 11. Concentration of HF as a function of PTFE fraction in sample material mixture, compared with the horizontal lines which depict wire insulation samples' average HF production over multiple replicates.

Effect of Fuel Preparation on Smoke Aerosol

It was observed that the aerosol mass concentration was approximately equal for a 100% PTFE pellet in the February/March testing and the loose ground PTFE test in September. This can be attributed to the nature of ground PTFE, which does not hold its pellet shape very well in spite of 10,000 psi of the pellet press. Thus the pellet process was never effective on that material. September testing showed the effect of the commercial 100 μm PTFE powder which makes 1/3 more aerosol mass concentration than the ground PTFE. The ground PTFE had granules that were much larger than 100 μm, as can be seen in the unburned fuel samples in Figure 3. The most significant effect of fuel preparation on aerosol output was with Kapton, where it was seen that the granulated Kapton produced five times more aerosol mass concentration than the Kapton film squares, which can be attributed to more surface area in granulated Kapton. The wire insulation was changed between the two test campaigns, and the average aerosol mass concentration in February/March was 0.013 g/m^3 but the September test version of insulation averaged 0.050 g/m^3.

C. Excessive Production of HF from Wire Insulation Compared to PTFE/Kapton blends

Figure 12 shows the production of HF and HCN from a variety of PTFE and Kapton blends (two-component mixture only) as a function of blend fraction in the "loose mix". Both optical PAS and electrochemical CSA-CP sensors are in qualitative agreement on the production of HCN as a function of Kapton fraction. There is an interesting and unexpected drop in measured HCN levels with pure Kapton (0.0 PTFE fraction) indicated by both sensors. The HF signal determined optically shows a like drop off in pure PTFE (1.0 fraction) relative to blends with even a small amount of Kapton (0.9 PTFE). However, that is likely caused by the lack of available hydrogen in pure PTFE resulting in a reduction in HF production relative to other, undetermined, fluorine containing combustion products. There is also an anomalous drop in HF production at 0.5 PTFE fraction which showed up in the two

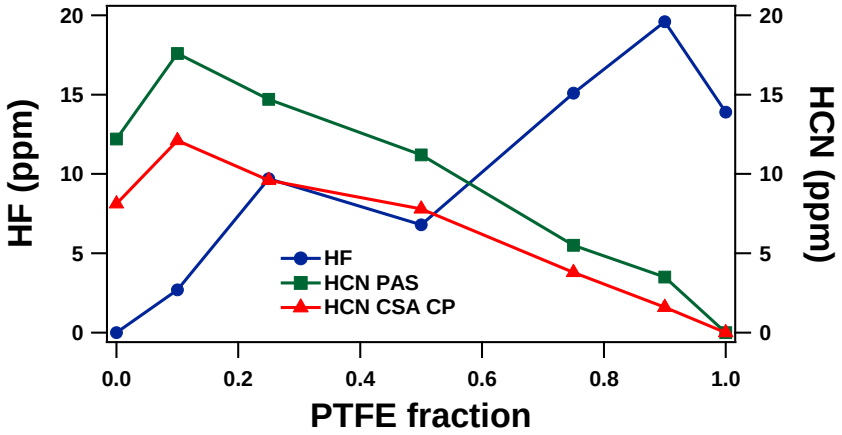

Figure 12. Production of HF and HCN as a function of PTFE fraction in sample material mixture.

separate optical sensor HF measurements. A possible explanation is that the 0.5 PTFE fraction measurements were made at the beginning of the testing regimen before the test chamber surfaces could have become passivated towards reactive gases. Nonetheless, the data show a fairly monotonic increase in HF with PTFE fraction and monotonic increase in HCN with Kapton fraction.

D. Sample Mass Loss

The residue from burned samples was weighed and recorded. A complete mass balance of the pyrolysis process was not attempted, however, the general trends in mass loss can give insight into the fire signature of various materials. The aerosol mass concentration in the exposure chamber was nearly constant throughout the heating cycle after the initial temperature ramp. Thus, an approximate total aerosol mass could be calculated from the mass concentration recorded with the known volume of the exposure chamber. Refer to Appendices E and F for the estimated mass of particles and ash mass from each test, and Figure 4 for photographs of the sample remains.

Ash mass was significantly affected by pelletization for Kapton. Loose samples had an average ash mass that was 15 to 30 times as large as the pelletized Kapton. Circuit board ash mass was larger than most other materials since the substrate FR-4 is designed to char, not combust. The combined ash mass and estimated aerosol mass

account for more than 70% of the initial sample weight, which is unusual compared to most materials tested. Nomex samples had nearly equal ash mass and estimated aerosol mass. Teflon samples had the smallest ash mass remaining after testing, with the average remaining mass only 16% of the original mass (0.5 g sample).

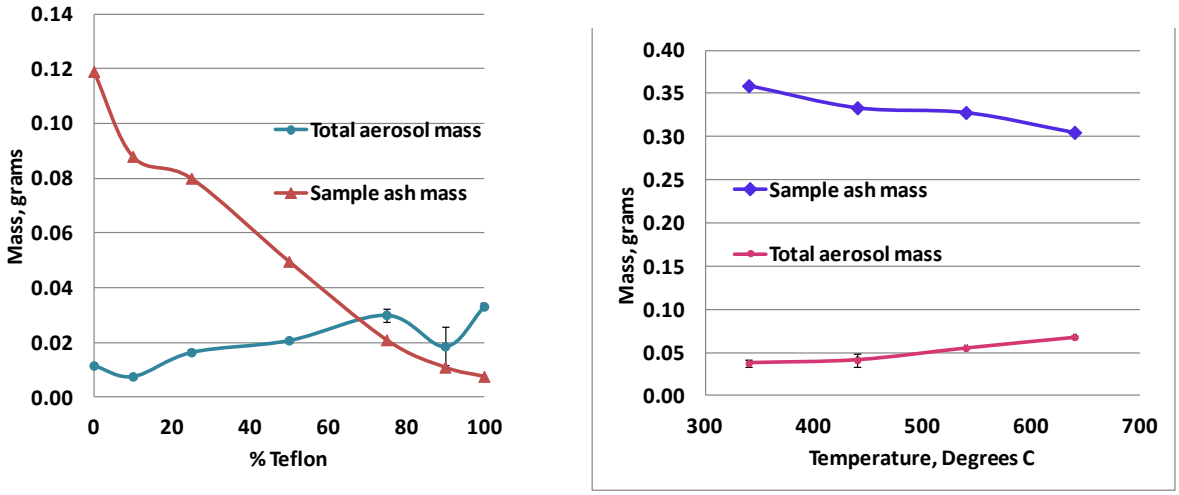

Figure 13. Mass accounting plots for Teflon/Kapton mixture tests (left) and granulated circuit card tests as a function of temperature for September tests. Error bars on aerosol mass represent one standard deviation.

The Teflon aerosol had a higher aerosol number concentration than most materials, but is made up of much smaller particles which filled the TEOM filter, necessitating higher dilution ratios and frequent filter changes. The right plot in Figure 13, shows that the total aerosol mass increases as the percentage of Teflon in the Teflon/Kapton mixture increases, and the sample ash mass decreases as the percentage of Teflon increases. This is an expected trend which is also evident in the circuit card graph on the left in Figure 13. Aerosol mass increases with increasing temperature, and there is a corresponding decrease in sample ash mass with increasing temperature. The error bars on the total aerosol mass represent one standard deviation in the mass measurement, which demonstrates that the repeatability of the heating and smoke generation between replicates was very good.

E. Improvements in Testing Methods and Results Between the Two Test Campaigns

Improvements between the two test campaigns were predominantly in the repeatability of the measurements. This was mostly accomplished by eliminating the standard mix which was fraught with variability in the grinding process of the constituent materials, as well as in the pellet preparation process. For the September test campaign we focused primarily on 640^{o} C furnace temperature to produce more replicates in one week's worth of testing. Future improvements will be made in the testing process, including ensuring that the acid gases have been sufficiently purged from the exposure chamber between runs. One method to control this is to incorporate a bake-out of the furnace between runs or more "air out" time between runs. Randomization in the order of the fuels may improve this as well, since the baseline HF concentration may be very small between different fuels instead of building up steadily when burning HF-producing samples all in succession. It has been observed that the first run of the day is often different, for example, CO is low for first fuel, first run of the day. HCl also did not return to zero between tests (this may take such a long time to accomplish that it would preclude the aggressive test schedule that is typically desired). A proposed solution is to subtract off a baseline value for subsequent tests. The electrochemical based devices are slow to rebaseline even in fresh air. We also noted that Nomex emits prolific chemical and particulate combustion products. Burning it first in the test campaign had consequences. Next time, Nomex will be burned on the last day.

Aerosols are notoriously difficult to generate consistently, particularly smoke aerosols. The February/March tests had very large ranges of aerosol mass concentration measurements, with the standard mix and 100% Teflon varying by a factor of 10 for the same temperature tests. There was a significant improvement in repeatability at the September testing where the focus was to improve this aspect of testing and to perform more replicates of the same tests. Over half of the standard deviations of the aerosol mass concentration measurements were less than 10% of the average values. The least repeatable materials in terms of mass concentration were the blend of circuit board

and PVC, the 90%-10% Teflon-Kapton mix and the Kapton squares, which differed by a factor of two at the most. Aerosol number concentration varied by a factor of two to four for Teflon, the standard mix and 25%-75% Teflon-Kapton, at the February/March testing with the other materials having much better repeatability, but the best improvement was the September testing with only two fuels having a standard deviation which was greater than 10% of the average value. Teflon has proven to be the most difficult material in terms of aerosol measurement repeatability. The improvement in aerosol measurements can be attributed to several practices, including careful fuel preparation, improved timing of procedural steps (Table 3), using loose fuel rather than pellets and, in particular, elimination of the standard mix.

V. Conclusion

Ongoing testing of gas sensors at WSTF contributes to the development of fire detection systems and post-fire cleanup monitoring equipment. Characterization of the gas and aerosol fire signatures of these polymers has contributed to the goal of providing a consistent and well-understood fire challenge for sensor testing, as well as validating the requirements and informing the design for the eventual suite of instruments that will make up the next generation spacecraft fire detection system. One notable conclusion is the significant production and persistence of acid gases HF and HCL in the chamber from a relatively small amount of fuel (0.5g). This result weighs heavily in the design of the next generation combustion product monitor which will eventually replace the aging CSA-CPs on International Space Station. A review of the volatile organic compounds results (GC/MS data) should yield interesting findings as well. Progress in testing and lessons learned have been noted for improving future testing campaigns. A future direction which merits its own study is an exclusive detailed study of HF production from fluoropolymer pyrolysis, looking specifically at the role of proton donors. Further, follow-up testing to investigate aspects of sensor system performance, both in simple gas mixtures and complex combustion environments, is warranted to better evaluate the capabilities of an individual sensor system.

Appendices

Appendix A. Carbon Monoxide data from all instruments in the February/March Test (in ppm)

Run#	Fuel	T/C	Ignite?	CSA-CP	Draeger	Vista COMA	Makel Fixed-L	Makel Fixed-H	Makel Port-L	Makel Port-H	WSTF PacIII	Avg	Std Dev
1	Std Mix	540	N	123	116	116	90	120	107	85	--	108	15
2	Std Mix	540	Y	47	46	44	53	50	55	49	--	49	4
4	Std Mix	540	N	106	100	98	109	103	107	107	108	105	4
5	Std Mix	540	Y	71	70	64	72	75	67	73	73	71	4
28	Std Mix	430	N	41	40	39	39	48	38	39	41	41	3
33	Std Mix	340	N	86	82	85	76	88	69	74	24	80	7
39	Std Mix	640	N	55	52	53	46	83	57	42	40	54	13
3	PFPI Wire Ins	540	N	109	106	106	109	117	115	111	92	110	4
6	PFPI Wire Ins	640	N	95	94	98	100	88	91	96	99	95	4
7	PFPI Wire Ins	540	N	186	182	177	200	180	184	157	194	183	13
21	PFPI Wire Ins	640	N	98	96	102	118	107	82	108	112	103	11
29	PFPI Wire Ins	640	N	98	96	99	109	110	88	110	101	101	8
31	PFPI Wire Ins	640	N	94	90	95	102	114	106	134	95	99	8
35	PFPI Wire Ins	540	N	130	126	128	127	145	116	151	88	132	12
8	Circuit Brd	540	N	24	26	23	23	25	27	35	25	26	4
10	Circuit Brd	640	N	40	38	37	39	39	33	32	39	37	3
23	Circuit Brd	640	N	36	36	39	39	34	35	22	37	37	2
27	Circuit Brd	340	N	37	36	38	27	39	25	< 20	38	34	6
34	Circuit Brd	430	N	33	30	31	27	< 20	28	24	34	30	3
9	100% TFE	540	N	5	0	5	6	< 20	8	< 20	5	5	3
15	100% TFE	640	N	10	8	9	9	< 20	8	< 20	7	9	1
20	100% PTFE	540	N	3	0	nd	4	< 20	5	< 20	0	3	2
30	100% TFE	640	N	9	6	7	2	< 20	9	< 20	7	7	3
42	100% TFE	640	N	8	6	6	5	< 20	2	< 20	12	6	3
22	90%T/10%K	640	N	19	20	20	16	< 20	18	< 20	19	19	2
36	90%T/10%K	640	N	34	34	37	30	< 20	32	< 20	24	32	4
14	75%T/25%K	540	N	9	8	8	11	< 20	12	< 20	8	9	2
19	75%T/25%K	640	N	42	40	37	42	41	39	44	42	41	2
32	75%T/25%K	640	N	32	30	31	31	23	28	48	31	32	7
12	50%T/50%K	540	N	18	16	14	17	< 20	18	< 20	17	17	2
17	50%T/50%K	640	N	72	70	69	72	64	69	74	74	71	3
25	50%T/50%K	640	N	52	54	55	46	37	62	73	56	54	11
13	25%T/75%K	540	N	15	14	13	15	< 20	13	< 20	14	14	1
18	25%T/75%K	640	N	118	112	109	113	114	123	122	122	117	5
38	25%T/75%K	640	N	79	74	79	63	83	72	93	35	78	9
43	25%T/75%K	540	N	218	212	213	200	231	86	37	28	215	11
24	10%T/90%K	640	N	98	94	103	102	108	96	109	102	102	5
37	10%T/90%K	640	N	106	104	110	113	119	84	97	17	105	11
11	100%Kapton	540	N	135	130	134	135	134	138	135	135	135	2
16	100%Kapton	640	N	156	150	153	152	150	152	152	162	153	4
26	100%Kapton	640	N	129	124	133	117	135	124	117	132	126	7
40	100%Kapton	540	N	18	16	14	38	< 20	7	< 20	109	19	12
41	100%Kapton	540	N	169	162	162	155	181	135	163	137	158	16

Shading denotes anomaly due to run sequence error or inadvertent (self) ignition (omitted from calculations)

XX Boxed values are omitted from average and standard deviation calculation. Conclusions on sensor performance should not be drawn at this time until further analysis is performed.

Appendix B. HCN and acid gas data from all instruments in February/March Test (in ppm)

				HCN						HCL				HF					HX	HBr
Run#	Fuel	T/C	Ignite?	Draeger	CSA-CP	PAS	PacIII	Avg	Std Dev	CSA-CP	Wet Trap	Avg	Std Dev	HF ii	HF iii	Wet Trap	Avg	StdDev	PacIII	Wet Trap
1	Std Mix	540	N	2.2	1.2	2.4	--	2	0.6	16	--	--	--	0.22	0	--	0.1	0.2	--	--
2	Std Mix	540	Y	0.7	0.2	0.9	--	1	0.4	3.7	--	--	--	2.1	4.3	--	3.2	1.6	--	--
4	Std Mix	540	N	2.5	1.4	2.7	4	3	1	15.1	1.4	--	--	0.2	0	0.4	0.2	0.2	0	0
5	Std Mix	540	Y	1.0	0.5	1.3	1.5	1	0.4	1.2	1.5	1.4	0.2	1.3	1.3	3.3	2.0	1.2	5.2	0
28	Std Mix	430	N	1.4	0.3	0.8	4.3	2	2	9.5	--	--	--	0.2	0.4	--	0.3	0.1	0.9	--
33	Std Mix	340	N	1.8	1.3	2.1	3	2	1	6.7	0.8			0	0	0.3	0.1	0.2	0	0
39	Std Mix	640	N	1.5	0.5	0.8	3.4	2	1	14.8	3.2			0.4	0.2	1.2	0.6	0.5	0.5	0.1
3	PFPI Wire Ins	540	N	2.7	1.8	3.2	6.7	4	2	5.4	2.9	4.2	1.8	16.5	21.7	33.8	24	8.9	0	0
6	PFPI Wire Ins	640	N	0.8	0.5	1	1.4	1	0.4	5.1	4.9	5.0	0.1	6.5	7.2	121	6.9	0.5	29	0.1
7	PFPI Wire Ins	540	N	0.8	0.5	1.1	1.4	1	0.4	3.8	0.8	2.3	2.1	11.5	14.2	26.9	17.5	8.2	> 30	0
21	PFPI Wire Ins	640	N	0.8	0.6	0.8	1.2	1	0.2	0.8	0.1	0.5	0.5	12.5	10.7	34.5	19.2	13.3	> 30	0
29	PFPI Wire Ins	640	N	1.2	0.5	0.8	3.1	1	1	4.0	0.6			11.0	10	27.9	16.3	10.1	16.7	0.1
31	PFPI Wire Ins	640	N	1.2	0.6	1	2	1	1	2.2	0			8.4	6.3	3.4	6.0	2.5	19.5	0
35	PFPI Wire Ins	540	N	1.3	1.1	1.3	3.2	2	1	5.3	0.2			11.0	10.7	12.7	11.5	1.1	19.1	0
8	Circuit Brd	540	N	0.6	0.1	nd	1.6	1	1	14.1	0.6			0.6	0.9	4	1.8	1.9	2.5	1.7
10	Circuit Brd	640	N	0.7	nd	nd	2.1	1	1	18.5	0.8			1.0	0.5	7.5	0.75	0.4	1.5	4.9
23	Circuit Brd	640	N	0.4	0.1	0.4	1.1	0	0.4	17.8	0.3			1.4	1.0	7.8	1.2	0.3	5.2	4.5
27	Circuit Brd	340	N	1	0.1	nd*	2.8	1	1	14.1	--			0.6	0.5	--	0.6	0.1	< 0.1	--
34	Circuit Brd	430	N	0.8	0.1	nd	2	1	1	25.5	0.2			0.2	0	0.9	0.4	0.5	0	1.0
9	100% TFE	540	N	0.2	0.1	nd	1.6	1	1	3.4	1			3.9	6.9	186	5.4	2.1	21	0.4
15	100% TFE	640	N	0	nd	nd	0.8	0	1	1.3	0			2.9	4.1	146	3.5	0.8	27	0
20	100% PTFE	540	N	0.2	0.2	nd	0.2	0	0.0	0.2	0.1			1.3	3.5	84.8	2.4	1.6	8.3	0
30	100% TFE	640	N	0	0.1	0.8	0.8	0	0.4	2.1	0			3.5	6.4	125	5.0	2.1	14.4	0
42	100% TFE	640	N	0	nd	1.4	0	0	1	1.2	0.6			1.6	3.3	37.3	2.5	1.2	8.8	0
22	90%T/10%K	640	N	0.8	0.3	0.9	0	0	0.4	0.6	0			3.9	4.4	139.2	4.2	0.4	25	0
36	90%T/10%K	640	N	1	0.5	1.4	2.5	1	1	2.8	0.2			3.9	6.4	37.6	5.2	1.8	0	0.1
14	75%T/25%K	540	N	0	nd	nd	0.8	0	1	1.2	0.3			2.5	3.4	27.3	3.0	0.6	19.6	0
19	75%T/25%K	640	N	2.2	1.1	2.6	3.3	2	1	1.2	0.2			5	6.5	37	5.8	1.1	27.4	0
32	75%T/25%K	640	N	1.7	1.0	2.9	2.8	2	1	2.1	--			5	5.6	--	5.3	0.4	--	--
12	50%T/50%K	540	N	0.6	nd	0.4	1	1	0.3	1.3	0.4			2.2	2.4	73.4	2.3	0.1	11.2	0
17	50%T/50%K	640	N	3.6	2.7	4.5	5.5	4	1	2.1	0.4			3.9	5.3	71.3	4.6	1.0	21.8	0
25	50%T/50%K	640	N	2.6	2.3	3.3	3.4	3	0.5	2.6	0.2			3.9	4.5	26.7	4.2	0.4	14.3	0
13	25%T/75%K	540	N	0	nd	nd	0.8	0	1	1.0	0.2			1.2	1.0	17.4	1.1	0.1	8.4	0
18	25%T/75%K	640	N	3.8	3.0	5	5.7	4	1	1.9	0.3			2.9	2.6	38.1	2.8	0.2	15.5	0
38	25%T/75%K	640	N	1.7	1.5	2	2.6	2	0.5	0.9	0.3			1.8	1.7	19.1	1.8	0.1	4.5	0
43	25%T/75%K	540	N	7.5	7.9	11.8	11.8	10	2	3.2	0.2			5.2	6	9	6.7	2.0	8.8	0
24	10%T/90%K	640	N	1.8	1.4	2.2	1.1	2	0	3.3	0.1			1.2	1.2	4.9	2.4	2.1	4	0
37	10%T/90%K	640	N	2.7	2.8	3.8	5.1	4	1	3.1	0.7			1.7	1.5	1	1.4	0.4	0	0.1
11	100%Kapton	540	N	4.2	3.4	5.6	5.9	5	1	3.3	0.2			0	0	0.4	0.1	0.2	0	0
16	100%Kapton	640	N	5.3	4.2	7.2	7.7	6	2	3.6	0.2			0.5	0.5	4.1	1.7	2.1	3.5	0
26	100%Kapton	640	N	3.0	2.6	3.9	4.9	4	1	2.5	0.1			0.2	0	0.7	0.3	0.4	1	0
40	100%Kapton	540	N	0.9	0.3	0.5	2	1	1	2.1	0			0	0	0.8	0.3	0.5	0	0
41	100%Kapton	540	N	5.8	5.6	8	9.2	7	2	3.4	0.1			0	0	0.4	0.1	0.2	0	0

Shading denotes anomaly due to run sequence error or inadvertent (self) ignition (omitted from calculations)

XX Boxed values are omitted from average and standard deviation calculation. Conclusions on sensor performance should not be drawn at this time until further analysis is performed.

Appendix C. Carbon Monoxide data from all sources for the September 2012 test (in ppm)

	Fuel	Temp	Date	Time	Ash		Draeger	Vista	Makel	Makel	Makel	Makel	WSTF	Run	Run	Fuel
Run #	0.5 g	C		local	g	CSA-CP	Xam5600	COMA	Fixed-L	Fixed-H	Port-L	Port-H	PacIII	Avg	Std Dev	Stats
1	Nomex	640	10-Sep	2:44	0.028	89	84	87	83	92	98	154	92	89	5	
2	"	"	"	3:11	0.046	118	112	129	125	103	152	110	127	122	15	
3	"	"	"	3:34	0.045	119	116	161	118	105	146	114	130	126	19	
4	"	"	"	4:00	0.014	92	92	121	92	113	90	99	104	100	11	
5	"	"	"	4:23	0.042	100	102	116	112	127	55	99	111	110	10	
6	Nomex	640	11-Sep	8:54	0.153	65	60	52	65	101	68	96	68			
7	"	"	"	9:15	0.091	105	100	87	93	108	102	84	113	99	10	
			excl #6	Avg		104	101	117	104	108	118	101	113			**108**
			excl #6	StdDev		13	12	28	17	12	29	12	14			**18**
8	M22759 ins	640	"	9:36	0.046	53	54	44	47	76	32	70	58			
9	"	"	"	10:06	0.021	76	78	59	82	81	74	85	82	77	8	
10	"	"	"	10:30	0.017	72	72	55	83	73	79	76	79	74	8	
11	"	"	"	10:53	0.021	78	80	61	90	65	59	62	85	73	12	
12	"	"	"	11:16	0.030	68	72	56	90	69	75	70	78	72	10	
13	"	"	"	11:37	0.017	72	76	60	90	69	75	70	82	74	9	
			excl #8	Avg		73	76	58	87	71	72	73	81			**74**
			excl #8	StdDev		4	4	3	4	6	8	9	3			**9**
14	PTFE granules	640	"	2:25	0.041	9	14	10	7	8	11	3	14	10	3	
15	"	"	"	2:48	0.014	10	14	9	9	3	9	5	14	10	3	
16	"	"	"	3:13	0.010	4	8	5	6	7	11	5	7	7	2	
17	"	"	"	3:38	0.015	8	12	8	12	10	14	7	11	10	2	
18	Kapton chips	640	"	4:07	0.227	266	268	215	295	226	206	205	285	246	37	
19	"	"	"	4:31	0.278	233	224	187	244	218	108	128	259	228	25	
20	"	"	"	4:52	0.251	294	282	239	293	316	131	168	324	291	30	
21	Kapton powder	640	12-Sep	9:10	0.126	292	272	232	292	273	218	301	325	276	36	
22	"	"	"	9:36	0.112	272	270	211	261	301	218	214	389	250	35	
			All Kapton	Avg		271	263	217	277	267	214	240	316			**258**
				StdDev		25	23	20	23	44	7	53	49			**38**
23	PTFE powder	640	12-Sep	9:56	0	24	28	21	16	10	8	0	31			
24	"	"	"	10:16	0.006	7	12	6	7	8	5	8	10	8	2	
25	"	"	"	10:37	0.008	8	14	8	10	8	11	11	11	10	2	
26	"	"	"	10:56	0.009	9	14	10	12	8	11	11	12	11	2	
		All PTFE excl #23		Avg		8	13	8	9	8	10	8	11			**9**
				StdDev		2	2	2	2	1	3	3	2			**3**
27	PCB	340	12-Sep	12:42	0.366	11	14	10	8	15	--	--	13	13	2	
28	"	"	"	1:02	0.352	20	22	16	19	29	--	--	23	22	4	
29	"	440	"	1:22	0.344	23	26	19	26	32	--	--	26	25	4	
30	"	"	"	1:42	0.323	25	28	20	27	43	--	--	29	29	8	
31	"	540	"	2:07	0.321	28	30	22	29	39	--	--	31	30	5	
32	"	"	"	2:30	0.335	25	28	22	27	35	--	--	29	28	4	
33	"	640	"	2:50	0.308	36	38	27	43	40	--	--	40	37	6	
34	"	"	"	3:18	0.302	34	36	27	41	36	--	--	38	35	5	
	Shading denotes anomaly due to run sequence error or inadvertent (self) ignition; data excluded from statistics													PCB 640C Avg		**36**
XX	Boxed values are omitted from average and standard deviation calculation. Conclusions on sensor performance should not be drawn at this time until further analysis is performed.													PCB 640C StdDev		**5**

Appendix C continued … (concentrations in ppm)

Run #	Fuel 0.5 g	Temp C	Date	Time local	Ash g	CSA-CP	Draeger Xam5600	Vista COMA	Makel Fixed-L	Makel Fixed-H	Makel Port-L	Makel Port-H	WSTF PacIII	Run Avg	Run Std Dev	Fuel Stats
35	100% PVC	640	12-Sep	3:36	0.009	66	66	48	--	--	--	--	38	**60**	**10**	
36	50/50 P/K	640	13-Sep	8:38	0.046	246	230	249	240	182	58	315	270	258	31	
37	"	"	"	8:59	0.061	253	246	256	265	236	211	278	283	254	23	
38	"	"	"	9:18	0.111	80	80	80	85	143	113	186				
39	"	"	"	9:35	0.042	286	280	298	330	271	357	245	321	299	36	
				Avg		262	252	268	278	254	284	279	291			**271**
				StdDev		21	26	27	46	25	103	35	27			**36**
40	25/75 P/K	640	"	9:54	0.092	301	286	311	340	248	357	218	334	311	37	
41	"	"	"	10:12	0.074	378	356	398	419	344	378	288	426	373	45	
42	"	"	"	10:31	0.128	156	138	132	123	159	107	166	144			
43	"	"	"	10:54	0.074	370	346	386	361	333	297	249	422	346	54	
				Avg		350	329	365	373	308	344	269	394			**345**
				StdDev		42	38	47	41	53	42	28	52			**51**
44	10/90 P/K	640	"	12:29	0.088	392	370	415	353	180	182	202	436	393	33	
45	"	"	"	12:48	0.139	228	220	238	198	137	73	151	250			
46	"	"	"	1:06	0.088	440	414	464	414	309	202	323	480	406	66	
				Avg		416	392	439.5	384	309	--	323	458			**401**
				StdDev		34	31	35	43	--	--	--	31			**53**
47	75/25 P/K	640	"	1:32	0.031	138	134	148	117	126	38	128	154	135	13	
48	"	"	"	1:50	0.047	53	60	56	52	114	61	152	60			
49	"	"	"	2:10	0.011	95	94	103	89	94	98	112	107	99	8	
50	"	"	"	2:30	0.021	120	118	131	124	124	118	139	135	126	8	
				Avg		118	115	127	110	115	108	126	132			**119**
				StdDev		22	20	23	19	18	14	14	24			**18**
51	90/10 P/K	640	"	2:53	0.016	77	76	83	72	81	55	87	87	77	10	
52	"	"	"	3:12	0.007	73	72	78	69	71	63	61	81	71	7	
53	"	"	"	3:30	0.010	55	56	59	55	72	40	53	63	59	7	
				Avg		68	68	73	65	75	53	67	77			**68**
				StdDev		12	11	13	9	6	12	18	12			**12**
54	90/10 P/PVC	640	"	3:47	0.002	37	38	39	41	29	35	33	43	37	4	
55	"	"	"	4:06	0.002	24	26	28	31	33	29	31	30	29	3	
56	"	"	"	4:24	0.001	27	28	28	39	27	33	28	32	30	4	
				Avg		29	31	32	37	30	32	31	35			**32**
				StdDev		7	6	6	5	3	3	3	7			**5**
57	PCB+PVC1	640	14-Sep	8:33	0.297	47	44	49	46	56	0	67	49	51	8	
58	"	"	"	8:56	0.347	43	42	46	44	57	35	61	47	47	8	**52**
59	"	"	"	9:17	0.312	57	50	63	58	68	54	58	55	58	6	**8**
60	PCB+PVC2	640	"	9:39	0.303	55	52	--	61	73	50	59	59	58	8	**61**
61	"	"	"	10:05	0.301	62	62	65	69	72	47	61	69	63	8	**8**
62	PTFE/PVC2	"	"	10:28	0.004	34	36	38	29	27	29	33	40	**33**	**5**	

Shading denotes anomaly due to run sequence error or inadvertent (self) ignition; data excluded from statistics

XX Boxed values are omitted from average and standard deviation calculation. Conclusions on sensor performance should not be drawn at this time until further analysis is performed.

Appendix D. HCN and acid gas results for the Sep 2012 test (in ppm)

			HCN						HCL					HF					HX	HBr
Run	Fuel	T/C	Draeger	CSA-CP	PAS	PacIII	Avg	StdDev	CSA-CP	HCPM	Wet Trap	Avg	StdDev	HCPM	Hfiii	Wet Trap	Avg	StdDev	PacIII	Wet Trap
1	Nomex	640	5.7	5.7	8.4	6.7	7	2	20	nd	0.2			nd	nd	nd	nd	--	nd	
2	"	"	6.4	6.2	9.4	7.6	7	1	25	nd	nd			nd	nd	nd	nd	--	nd	
3	"	"	7.8	7.3	10.8	8.7	9	2	26	nd	0.3			nd	nd	nd	nd	--	nd	
4	"	"	5.4	5.3	7.3	6.3	6	1	26.5	nd	0.3			nd	nd	nd	nd	--	nd	
5	"	"	6.1	5.9	8.7	7.1	7	1	28	nd	0.4			nd	nd	nd	nd	--	nd	
6	"	"	6.0	5.8	8.1	7.2	7	1	18.1	nd	0.1			nd	nd	nd	nd	--	7.1	
7	"	"	8.1	7.8	10.4	9.5	9	1	25	nd	0.1			nd	nd	nd	nd	--	19.3	
		Avg	6.5	6.3	9.0	7.6		**7.3**												
		StDev	1.0	0.9	1.3	1.1		**1.5**												
8	M22759 ins	640	3.4	3.3	4.4	4.2	4	1	6.8	nd	0.0			7.1	4	9.2	7	3	29.4	
9	"	"	3.4	3.1	4.4	4.2	4	1	6.5	nd	1.4			8	6.5	11.2	9	2	30.0	
10	"	"	4.0	3.6	4.9	4.8	4	1	7.7	nd	1.2			10.5	8.8	27.9	10	1	30.0	
11	"	"	3.8	3.4	4.7	4.7	4	1	7.2	nd	0.1			12.3	11.3	20.5	15	5	30.0	
12	"	"	3.9	3.5	5	4.8	4	1	6.6	nd	0.1			13.3	12.2	24	13	1	27.6	
13	"	"	3.7	3.1	4.7	4.6	4	1	5.6	nd	0.1			12.8	14.2	13.9	14	1	30.0	
		Avg	3.7	3.3	4.7	4.6		**4.1**	6.7	nd	0.5			10.7	9.5	13.7		**11**	29.5	
		StDev	0.3	0.2	0.2	0.3		**0.6**	0.7	nd	0.6			2.6	3.8	4.9		**4**	1.0	
14	PTFE granules	640	nd	0.1	nd	0.6			1.3	nd				10.1	12.9		12	2	30	
15	"	"	nd	0	nd	0.3			1.3	nd	0.1			14.7	17.4	45.7	16	2	30	
16	"	"	nd	-0.2	nd	0.3			1.1	nd	0.1			8.6	15.1	21.6	15	7	0	
17	"	"	nd	-0.2	nd	0.2			1.2	nd				10.7	15.2		13	3	0	
18	Kapton chips	640	10.2	8.9	13.6	12.0	11	2	10	nd	nd			1.7	1.8	3.4	2	1	nd	
19	"	"	7.7	6.7	9.6	9.2	8	1	8.7	nd	nd			0.8	nd	1.4	1	nd	nd	
20	"	"	12.3	11.2	15.6	14.2	13	2	12.3	nd	0.2			0.6	nd	1.0	1	nd	nd	
21	Kapton powder	640	8.1	8.4	11.6	10.2	10	2	14	nd	nd			nd	nd				nd	
22	"	"	7.5	7.8	10.7	9.9	9	2	15	nd	nd			nd	nd				nd	
	all Kapton	Avg	9.2	8.6	12.2	11.1		**10.3**		nd	nd		**nd**					**1**		
		StDev	2.1	1.7	2.4	2.0		**2.4**										**0.8**		
23	PTFE powder	640	nd	0.1	nd	0.5			2.0	nd	0.1			7.2	7.6	14.6	10	4	17.6	
24	"	"	nd	-0.3	nd	0.4			1.4	nd	0.0			7	11.3	32.2	9	3	12.7	
25	"	"	nd	-0.1	nd	0.3			1.3	nd	0.2			9.5	14.4	24.5	16	8	17.3	
26	"	"	nd	-0.2	nd	0.1			1.3	nd	0.1			11.8	17.6	22.2	17	5	19.4	0.9
	all PTFE	Avg	nd	nd	nd	0.3				nd	0.1		**nd**	10.0	13.9	20.7		**13**	16.8	
		StDev				0.2								2.5	3.3	4.3		**5**	2.9	
27	PCB	340	nd	0.1	nd	0.3			10.2	nd	0.0			0.5	0.7		0.6	0.1	nd	nd
28	"	"	nd	0.1	nd	0.3			13.5	nd				0.3	0.7		0.5	0.3	nd	
29	"	440	nd	0.1	nd	0.3			17	nd	0.1			0.3	0.4	1.5	0.7	0.7	nd	1.8
30	"	"	nd	0.1	nd	0.4			16.2	nd	0.0			0.4	0.1	0.9	0.5	0.4	nd	0.8
31	"	540	nd	0.1	nd	0.4			17	nd	0.2			0.4	0.1	1.1	0.5	0.5	0.8	2.3
32	"	"	nd	0.1	nd	0.4			16.6	nd	0.1			0.4	0.5	1.0	0.6	0.3	0.9	2.2
33	"	640	nd	0.1	nd	0.5			19.8	nd	0.2			0.4	0.4	1.5	0.8	0.6	1.3	1.0
34	"	"	nd	0.1	nd	0.6			18	nd	0.1			0.4	0.3	1.2	0.6	0.5	0.9	1.0
		Avg						**nd**					**nd**			avg at 640C		**0.7**		1.0
		StDev														stdev at 640C		**0.5**		
	Shading denotes anomaly due to run sequence error or inadvertent (self) ignition; data excluded from statistics																			
XX	Boxed values are omitted from average and standard deviation calculation. Conclusions on sensor performance should not be drawn at this time until further analysis is performed.																			

Appendix D continued…. (concentrations in ppm)

			HCN						HCL					HF					HX	HBr
Run #	Fuel	T/C	Draeger	CSA-CP	PAS	PacIII	Avg	StdDev	CSA-CP	HCPM	Wet Trap	Avg	StdDev	HCPM	Hfiii	Wet Trap	Avg	StdDev	PacIII	Wet Trap
35	100% PVC	640	7.3	0.2	nd	8.4	4		> 99	252	59.9			4.4	6.3	14	8		> 30	0.4
36	50/50 P/K	640	5.9	6.2	8.7	7.6	7	1	6	0.6	0.6	0.6		3.3	3.3	19.3			4.7	0.2
37	"	"	8.9	8.2	11.6	9.3	10	1	6.6	0.6	0.5	0.6		6.5	6.9	21.6			9.0	0.1
38	"	"	3.5	3.3	4.5				7.7	0.4				5.3	6.1					
39	"	"	10.2	9.2	13.4	12	11	2	8.2	0.8	0.7	0.8		8.6	10.3	24.4			11.5	0.1
		Avg	8	7.9	11.2	9.6		**9.3**					**0.6**							0.1
		StDev	2	1.5	2.4	2.2		**2.3**					**0.1**							
40	25/75 P/K	640	8.9	8.2	12.2	10.4	10	2	9.5	nd	0.7			7.6	9.3	11.3			9.4	nd
41	"	"	11.8	10.4	16.2	13.6	13	3	10.5	nd	0.5			7.8	9.9	8.9			5.3	nd
42	"	"	4.1	4.1	5	4.4			6.2	nd	0.1			7.8	9.4	2.8			4.5	nd
43	"	"	11.6	10.4	15.6	13.1	13	2	10	nd	0.5			8.2	10	9.5			5.1	nd
		Avg	10.8	9.7	14.7	12.4		**11.9**										**9.2**		nd
		StDev	1.6	1.3	2.2	1.7		**2.5**										**1.2**		
44	10/90 P/K	640	11.8	11.2	15.9	13.4			9.1	nd	0.2			2.2	2.4	4.5			1.6	nd
45	"	"	7.2	7.0	9.6	8.2			6.9	nd	nd			2.4	2.7	2.4			1.7	nd
46	"	"	14.4	13.1	19.2	15.2			9.3	nd	0.1			2.5	3	3.3			1.7	nd
		Avg	13.1	12.2	17.6	14.3		**14.3**					**nd**					3.0		nd
		StDev	1.8	1.3	2.3	1.3		**2.5**												
47	75/25 P/K	640	5.5	4.6	7.2	6.0			4.8	nd	0.1			9.1	13.6	16.6			5.4	nd
48	"	"	2.8	2.4	3.7	3.2			3.7	0.8	0.6			10	13	20.1			6.8	nd
49	"	"	4.1	3.4	5.5	4.7			5	0.8	0.5			11.3	15.2	23.9			7.3	nd
50	"	"	4.3	3.7	5.7	4.9			5.7	0.4	0.4			14.3	18.7	23.9			9.0	nd
		Avg	4.6	3.9	6.1	5.2		**5.0**					**0.4**							nd
		StDev	0.8	0.6	0.9	0.7		**1.1**					**0.3**							
51	90/10 P/K	640	3.1	2.2	3.7	3.3			4.3	0.6	0.2			10	14.9	28.4			8.5	nd
52	"	"	2.7	1.6	3.7	3.1			4.9	0.4				15.3	21.4				10.5	nd
53	"	"	2.3	1.3	3.2	2.8			4.5	0.6				16.9	22.5				10.8	nd
		Avg	2.7	1.7	3.5	3.1		**2.8**					**0.5**							nd
		StDev	0.4	0.5	0.3	0.3		**0.8**					**0.2**							
54	90/10 P/PVC	640	0.6	0	nd	0.6			26.5	25	6.4			17.9	24	29.4			14.3	nd
55	"	"	0.6	0	nd	0.8			35	29.2	9.6			17.1	22.8	30.2			13.5	nd
56	"	"	0.6	0.1	nd	0.7			43	29.2	9.4			18.3	24	33			13.1	nd
		Avg	0.6	0.0	nd	0.7		**0.4**					**18.1**						13.6	nd
		StDev	nd	0.1		0.1		**0.3**					**10.8**						0.6	
57	PCB+PVC1	640	nd	0.2	nd	1.3			19	23	3.7			1.0	1.3	1.5			0.7	2
58	"	"	0.5	0.2	nd	1.5			35	28.4	5.1			1.0	1.1	1.3			0.8	1
59	"	"	0.6	0.2	nd	1.9			44.7	29.4				1.1	1.4				0.7	
		Avg						**0.8**												
		StDev						**0.7**												
60	PCB+PVC2	640	1.3	0.2	nd	2.5			97	62.2	21.3			1.3	1.7	4			2.5	3.7
61	"	"	1.4	0.2	nd	2.5			86.5	60	15.1			1.2	1.5	1.5			2.6	1.1
		Avg																		
		StDev																		
62	PTFE/PVC2	"	1.9	0.2	nd	2.5			99+	67.8				7.2	8.6				2.8	

Shading denotes anomaly due to run sequence error or inadvertent (self) ignition; data excluded from statistics

XX Boxed values are statistical outliers omitted from average and standard deviation calculation. Conclusions on sensor performance should not be drawn at this time until further analysis is performed.

Appendix E. Aerosol Mass Concentration and Ash Data for February/March 2012 Test

Feb/Mar 2012 TestDates	Test No.	Material	Temp, C	TEOM Mass Conc mg/m^3	TEOM Mass Conc g/m^3	Thermal Precipitator	Aerosol Number Concentration, #/cm^3	Estimated Mass of Particles, g	Ash Mass, g
2/27/2012	1	Std Mix	540	11.91	0.0119	Y		0.0074	0.0119
	2	"	540	65.09	0.0651	Y		0.0405	0.0651
Day 1	3	wire insulation	540	6.80	0.0068	Y		0.0042	0.0068
2/28/2012	4	Std Mix	540	106.52	0.1065	Y	4.90E+06	0.0664	0.1065
	5	"	540	67.01	0.0670	Y	4.33E+06	0.0417	0.0670
	6	wire insulation	640	14.42	0.0144	Y	3.31E+06	0.0090	0.0144
	7	"	540	10.16	0.0102		3.28E+06	0.0063	0.0102
	8	Circuit Bd	540	54.14	0.0541	Y	3.60E+06	0.0337	0.0541
	9	100% TFE	540	95.64	0.0956	Y	4.30E+06	0.0596	0.0956
	10	Circuit Bd	640	107.19	0.1072		4.53E+06	0.0668	0.1072
	11	100%Kapton	540	7.21	0.0072	Y	3.40E+06	0.0045	0.0072
	12	50%TFE 50% Kap	540	4.81	0.0048	Y	1.57E+06	0.0030	0.0048
	13	25%TFE 75%Kap	540	14.16	0.0142	Y	1.24E+06	0.0088	0.0142
	14	75%TFE 25%Kap	540	13.19	0.0132	Y	1.83E+06	0.0082	0.0132
	15	100% TFE	640	13.61	0.0136	Y	2.44E+06	0.0085	0.0136
	16	100%Kapton	640	12.84	0.0128	Y		0.0080	0.0128
	17	50%TFE 50% Kap	640	49.25	0.0492	Y	2.33E+06	0.0307	0.0492
	18	75%TFE 25%Kap	640	29.57	0.0296	Y	2.19E+06	0.0184	0.0296
Day 2	19	75%TFE 25%Kap	640	22.76	0.0228	Y	2.03E+06	0.0142	0.0228
2/29/2012	20	100% TFE	540	2.40	0.0024	Y	1.16E+06	0.0015	0.0024
	21	wire insulation	640	21.06	0.0211		2.41E+06	0.0131	0.0211
	22	90%TFE 10%Kap	640	8.35	0.0083		1.95E+06	0.0052	0.0083
	23	Circuit Bd	640	77.09	0.0771	Y	4.17E+06	0.0480	0.0771
	24	10%TFE 90%Kap	640	62.13	0.0621		2.44E+06	0.0387	0.0621
	25	50%TFE 50% Kap	640	25.73	0.0257	Y	2.04E+06	0.0160	0.0257
	26	100%Kapton	640	9.19	0.0092		2.24E+06	0.0057	0.0092
	27	Circuit Bd	340	110.96	0.1110	Y	3.80E+06	0.0691	0.1110
	28	Std Mix	430	96.95	0.0969	Y	2.35E+06	0.0604	0.0969
	29	wire insulation	640	16.83	0.0168	Y	2.85E+06	0.0105	0.0168
	30	100% TFE	640	10.78	0.0108		1.71E+06	0.0067	0.0108
	31	wire insulation	640	11.68	0.0117		2.21E+06	0.0073	0.0117
Day 3	32	75%TFE 25%Kap	640	24.09	0.0241		2.01E+06	0.0150	0.0241
3/1/2012	33	Std Mix	340	131.31	0.1313		4.27E+06	0.0818	0.1313
	34	Circuit Bd	430	95.82	0.0958		2.83E+06	0.0597	0.0958
	35	wire insulation	540	11.08	0.0111	Y	2.87E+06	0.0069	0.0111
	36	90%TFE 10%Kap	640	71.28	0.0713	Y	3.57E+06	0.0444	0.0713
	37	10%TFE 90%Kap	640	29.57	0.0296		2.16E+06	0.0184	0.0296
	38	25%TFE 75%Kap	640	21.91	0.0219	Y	1.62E+06	0.0136	0.0219
	39	Std Mix	640	49.61	0.0496		3.02E+06	0.0309	0.0496
	40	100%Kapton	540	2.40	0.0024		1.26E+06	0.0015	0.0024
	41	100%Kapton	540	7.21	0.0072		1.85E+06	0.0045	0.0072
	42	100% TFE	640	12.96	0.0130	Y	1.45E+06	0.0081	0.0130
Day 4	43	25%TFE 75%Kap	540	44.92	0.0449		2.39E+06	0.0280	0.0449

Appendix F. Particle mass concentration and ash data for the Sep 2012 Test

Note: Grey cells denote anomaly due to run sequence error or inadvertent self-ignition; omit from averages, or no data available for this test. No aerosol mass concentration data collected for runs 59-62

Sep 2012 TestDates	Test No.	Material	TEOM Mass Conc g/m^3	Avg Mass Conc, g/m^3	standard dev, g/m^3	Aerosol Mass Fraction below 1 µm	Aerosol Number Concentration,	Avg Number Conc, #/cm^3	standard dev, #/cm^3	Est mass of particles, g	Ash Mass (g)
9/10/2012	1	NOMEX	0.0774							0.0482	0.028
	2	"	0.0440	TP			4.82E+06			0.0274	0.046
	3	"	0.0718				4.52E+06			0.0447	0.045
	4	"	0.0647				4.85E+06			0.0403	0.014
	5	"	0.0727				4.55E+06			0.0453	0.042
Day 1	6	"	0.0639	(omit from avg)			5.62E+06			0.0398	0.153
9/11/2012	7	"	0.0622	TP			5.72E+06			0.0387	0.091
		average & st dev		**0.0655**	**0.0119**			**4.89E+06**	**4.87E+05**	**0.0408**	**0.044**
	8	wire insulation	0.0705	(omit from avg)			5.95E+06				0.046
	9	"	0.0559				4.29E+06			0.0348	0.021
	10	"	0.0435				4.07E+06			0.0271	0.017
	11	"	0.0493				3.96E+06			0.0307	0.021
	12	"	0.0478				4.29E+06			0.0297	0.030
	13	"	0.0542				3.91E+06			0.0337	0.017
		average & st dev		**0.0501**	**0.0050**			**4.10E+06**	**1.78E+05**	**0.0312**	**0.021**
	14	100% PTFE	0.0367			1	4.28E+06			0.0229	0.041
	15	"	0.0335			0.994	4.84E+06			0.0209	0.014
	16	"	0.0344			1	3.25E+06			0.0214	0.010
	17	"	0.0503			0.988	2.52E+06			0.0313	0.015
		average & st dev		**0.0387**	**0.0078**			**3.73E+06**	**1.04E+06**	**0.0241**	**0.020**
	18	kapton squares	0.0049			0.993	2.90E+06			0.0031	0.227
	19	"	0.0024			0.996	2.94E+06			0.0015	0.278
	20	"	0.0036			1	3.01E+06			0.0022	0.251
Day 2		**average & st dev**		**0.0036**	**0.0013**			**2.95E+06**	**5.58E+04**	**0.0023**	**0.252**
9/12/2012	21	granulated kapton	0.0179			0.982	4.41E+06			0.0112	0.126
	22	"	0.0194			0.984	4.32E+06			0.0121	0.112
		average & st dev		**0.0187**	**0.0011**			**4.36E+06**	**6.13E+04**	**0.0116**	**0.119**
	23	PTFE powder (100 um)	0.0173	(omit from avg)		0.982	3.30E+06				0
	24	"	0.0550			0.999	5.20E+06			0.0343	0.006
	25	"	no data			0.998	4.96E+06			no data	0.008
	26	"	0.0516			0.997	4.98E+06			0.0321	0.009
		average & st dev		**0.0533**	**0.0024**			**5.05E+06**	**1.32E+05**	**0.0332**	**0.008**
	27	340 PCB	0.0557			0.936	4.00E+06			0.0347	0.366
	28	"	0.0651	TP		0.928	4.12E+06			0.0406	0.352
		average & st dev		**0.0604**	**0.0066**			**4.06E+06**	**8.33E+04**	**0.0376**	**0.359**
	29	440 PCB	0.0580			0.922	5.43E+06			0.0361	0.344
	30	"	0.0742	TP		0.922	5.35E+06			0.0462	0.323
		average & st dev		**0.0661**	**0.0115**			**5.39E+06**	**5.58E+04**	**0.0412**	**0.334**
	31	540 PCB	0.0885	TP		0.922	6.20E+06			0.0551	0.321
	32	"	0.0885			0.923	5.88E+06			0.0551	0.335
		average & st dev		**0.0885**	**0.0000**			**6.04E+06**	**2.25E+05**	**0.0551**	**0.328**
	33	640 PCB	0.1070	TP		0.926	6.66E+06			0.0667	0.308
	34	"	0.1110			0.911	6.32E+06			0.0692	0.302
		average & st dev		**0.1090**	**0.0028**			**6.49E+06**	**2.43E+05**	**0.0679**	**0.305**
	35	PVC	0.1150			0.893	6.11E+06			0.0716	0.009
Day 3				0.1150				6.11E+06			

Appendix F. continued…

9/13/2012	36	50-50 teflon/kapton	0.0358			0.993	4.36E+06			0.0223	0.046
	37	(100 um teflon powder/	0.0252			0.988	3.82E+06			0.0157	0.061
	38	granulated kapton)	0.0364	(omit from avg)		0.993	4.03E+06				0.111
	39	"	0.0394			0.995	3.95E+06			0.0245	0.042
		average & st dev		**0.0334**	**0.0074**			**4.04E+06**	**2.83E+05**	**0.0208**	**0.050**
	40	25-75 teflon/kapton	0.0284			0.994	3.81E+06			0.0177	0.092
	41	(100 um teflon powder/	0.0254			0.991	3.75E+06			0.0158	0.074
	42	granulated kapton)	0.0252			0.988	3.66E+06			0.0157	0.128
	43	"	0.0270			0.993	3.55E+06			0.0168	0.074
		average & st dev		**0.0265**	**0.0015**			**3.69E+06**	**1.16E+05**	**0.0165**	**0.080**
	44	10-90 teflon/kapton	0.0129			0.996	3.29E+06			0.0080	0.088
	45	(100 um teflon powder/	0.0140	(omit from avg)		0.988	3.30E+06				0.139
	46	granulated kapton)	0.0117			0.993	3.76E+06			0.0073	0.088
		average & st dev		**0.0123**	**0.0008**			**3.52E+06**	**3.33E+05**	**0.0076**	**0.088**
	47	75-25 teflon/kapton	0.0498			0.996	3.18E+06			0.0310	0.031
	48	(100 um teflon powder/	0.0250	(omit from avg)		0.977	3.68E+06				0.047
	49	granulated kapton)	0.0440			0.996	3.80E+06			0.0274	0.011
	50	"	0.0512			0.996	3.29E+06			0.0319	0.021
		average & st dev		**0.0483**	**0.0038**			**3.42E+06**	**3.33E+05**	**0.0301**	**0.021**
	51	90-10 teflon/kapton	0.0171			1	3.19E+06			0.0106	0.016
	52	(100 um teflon powder/	0.0349			0.997	3.48E+06			0.0218	0.007
	53	granulated kapton)	0.0378	0.0364	0.0020	0.995	3.93E+06			w/o outlier (#51	0.010
		average & st dev		**0.0299**	**0.0112**			**3.54E+06**	**3.71E+05**	**0.0187**	**0.011**
	54	90-10 teflon/PVC	0.1113			0.969	4.33E+06			0.0693	0.002
	55	(100 um teflon powder/	0.1386			0.944	4.35E+06			0.0863	0.002
	56	granulated PVC)	0.1301			0.945	5.97E+06			0.0810	0.001
Day 4		**average & st dev**		**0.1343**	**0.0060**			**4.88E+06**	**9.42E+05**	**0.0837**	**0.002**
9/14/2012	57	PCB+PVC1	0.0497				5.99E+06				
	58	"	0.1110				5.88E+06				
	59	"					5.82E+06				
		average & st dev		**0.1110**	**0.0433**			**5.90E+06**	**8.62E+04**		
	60	PCB+PVC2					5.83E+06				
	61	"					4.66E+06				
Day 5		**average & st dev**						**5.25E+06**	**8.23E+05**		

Acknowledgments

Certain commercial entities, equipment, or materials may be identified in this document in order to describe an experimental procedure or concept adequately. Such identification is not intended to imply recommendation or endorsement by the National Aeronautics and Space Administration, nor is it intended to imply that the entities, materials, or equipment are necessarily the best available for the purpose.

References

1. Ruff, G. A., Greenberg, P. S., Mudgett, P. D., Hornung, S. D., Pilgrim, J. S., Vakhtin, A. B, "Towards the Ientification of Chemical Markers for Spacecraft Post-fire Cleanup," 41st International Conference On Environmental Systems, SAE, Portland, OR, 17-21 July 2011, AIAA 2011-5052.
2. Sribnik,F., Birbara, P.J., Faszcza, J. J., and Nalette, T. A., "Smoke and Contaminant Removal System for Space Station," SAE Paper 901390, 20th Intersociety Conference on Environmental Systems, Williamsburg, VA, July 9-12, 1990.
3. Pilgrim, Jeffrey S. "Advanced Fire Detector for Space Applications," NASA Tech Briefs, 36, No. 6 (2012), 90.
4. Pilgrim, Jeffrey S. "Rugged, Portable, Real-Time Optical Gaseous Analyzer for Hydrogen Fluoride," NASA Tech Briefs, 36, No. 10, (2012), 25.
5. Hunter, G. W., Xu, J. C., Biaggi-Labiosa, A. M., Ward, B., Dutta, P., and Liu, C. C., "Smart Sensor System for Spacecraft Fire Detection and Air Quality Monitoring," 41st International Conference On Environmental Systems, SAE, Portland, OR, 17-21 July 2011, AIAA 2011-5021.
6. Hunter, G. W., Greenberg, P. S., Xu, J. C., Ward, B., Makel, D., Dutta, P., and Liu, C. C., "Miniaturized Sensor Systems for Early Fire Detection in Spacecraft," 39th International Conference On Environmental Systems, SAE, Warrendale, PA, 12-16 July 2009, 09ICES-0335.